APPARATUS AND TECHNIQUE FOR THE EVALUATION OF MAGNETIC CONDITIONING AS A MEANS OF RETARDING WAX DEPOSITION IN PETROLEUM PIPELINES

By

JOHNNY LAMAR EVANS JR.

A DISSERTATION PRESENTED TO THE GRADUATE SCHOOL OF THE UNIVERISTY OF FLORIDA IN PARTIAL FULFILLMENT OF THE REQUIREMENTS FOR THE DEGREE OF DOCTOR OF PHILOSOPHY

UNIVERSITY OF FLORIDA
1998

Copyright 1998

by

Johnny Lamar Evans Jr.

For my wife, Jeannie

ACKNOWLEDGEMENTS

An individual's success is not just dependent upon his efforts alone, but also upon the level and quality of support from those around him. Realizing this, I want to thank those who have contributed to my education at the University of Florida and helped to make this work a success. First, I want to thank my mentor, Dr. Samuel Colgate, for his never-ending support and encouragement throughout this project. I am blessed to have worked with such an outstanding engineer, chemist, and teacher.

One of the many benefits of graduate school is the opportunity to work with a variety of talented students. I would like to thank those individuals for their encouraging, comedic, and sometimes scientific, discussions about magnetic conditioning. In particular I would like to thank the past members of the Colgate research group--Dan Tatro, Vu Thieu, Karl Zachary, and Troy Halvorsen--and Heather Wiemer.

The design and development of the apparatus was made possible by the hard work and dedication of several

individuals. Special thanks goes to Dr. Evan House for his assistance with the programming and instrument design, and Steve Miles for his work in designing and fabricating the electronics. The assistance of Joe Shalosky and Todd Prox in fabrication of the apparatus was extraordinary. Their dedication to expert craftsmanship, patience in teaching, and friendship are greatly appreciated.

Finally, I would like to thank my friends and family for their support and encouragement throughout my academic career. In particular, I would like to thank my wife for standing by my side and helping me to reach this goal. Congratulations Jeannie! You have obtained your P.H.T. (Putting Hubby Through).

TABLE OF CONTENTS

ACKNOWLEDGEMENTS iv

ABSTRACT viii

CHAPTERS

1 INTRODUCTION 1

2 PARAFFINIC CRUDES 6

Characteristics of Paraffinic Crudes 6
Crystal Morphology 7
Temperature Effects 9
Wax Deposition 11
Wax Remediation Tactics 13
Magnetic Fluid Conditioners 16

3 EXPERIMENTAL 18

Pipeline 19
Filter 22
Cooling Stage 26
Isothermal Stage 27
Digital Flow Meters 32
Wax Deposition Stage 36
Stainless Steel Trough 36
Teflon Plate and Aluminum Top Plate 37
Peripheral Parts 37
Magnetic Fluid Conditioners 42
Oil Samples 45
Measurement Hardware and Interfacing 45

4 EXPERIMENTAL PROCEDURE 49

Pipeline Assembly and Thermal Flow
Data Acquisition 49
Magnetic Conditioning Procedure 51

Wax Deposition Procedure and Hardness Testing 51

5 RESULTS 54

Thermal Flow Profiles Before Magnetic Conditioning 55
Magnetic Conditioning Data 55
Wax Hardness Analysis 56

6 DISCUSSION AND CONCLUSION 73

Sensitivity of Digital Flow Meters 73
Possible Design Improvements 75
The Effects of Magnetic Conditioning 77

APPENDICES

A DIGITAL FLOW METER CIRCUIT 84

B TEMPERATURE CONTROL 86

C COMPUTER PROGRAM 90

REFERENCES 109

BIOGRAPHICAL SKETCH 111

Abstract of Dissertation Presented to the Graduate School of the University of Florida in Partial Fulfillment of the Requirements for the Degree of Doctor of Philosophy

APPARATUS AND TECHNIQUE FOR THE EVALUATION OF MAGNETIC CONDITIONING AS A MEANS OF RETARDING WAX DEPOSITION IN PETROLEUM PIPELINES

By

Johnny Lamar Evans Jr.

August 1998

Chairperson: Dr. Samuel O. Colgate
Major Department: Chemistry

For many years the crystallization and deposition of n-paraffins has hampered the harvesting, transportation, and processing of crude oil. Many methods have been developed in an attempt to inhibit wax deposition (e.g. heat conservation, chemical treatments, and pipe coatings), but with little success. In the early 1980s, during the height of this search for reliable and affordable wax management methods, magnetic fluid conditioners became widely available to the industry. Claims that passive magnetic fields inhibit wax crystallization and deposition are copious; however, such statements have been made without the support of clear scientific evidence. The

focus of this research has been to illuminate the subject and evaluate the effect of magnetic fields on the deposition of wax in a flowing system.

A novel instrument was developed for the simultaneous monitoring of two identical flowing fluids, identical except for exposure of one of them to magnetic fields. In addition, a wax deposition stage was developed to facilitate the deposition wax on nickel and Teflon surfaces. The results show a depression of the wax deposition temperature of some fluid flows exposed to magnetic fields, suggesting that magnetic conditioners may in fact affect the crystal morphology or deposition mechanism of wax.

CHAPTER 1
INTRODUCTION

People in developed countries have come to expect abundant energy on demand, and petroleum fuels have long provided a large source of that energy; however, current land based and shallow-water offshore wells will not be able to meet all demands of the future. Consequently, the petroleum industry has placed an emphasis on exploring and harvesting the yet untouched, vast petroleum reservoirs lying offshore in deep-sea beds. Such exploration and subsequent production, however, are costly and difficult.

Harvesting crude oil from deep-water wells involves drilling into the oil bearing formation a considerable distance from a production platform and transporting the crude to the platform by a system of pipelines and pumps called tie-backs. As the industry continues to explore deeper parts of the ocean, single production platforms will be supplied by several tiebacks with hundreds of miles of networked pipeline. The engineering challenge of constructing such extensive systems thousands of feet below

the surface is obvious, but this is not the only obstacle project designers must overcome.

The design and installation of successful wells requires extensive studies of the composition and behavior of the reservoir fluids, and these are variable from reservoir to reservoir and in a single reservoir over its production lifetime. Petroleum companies invest heavily of time and resources to determine the composition of reservoir crudes in an attempt to facilitate prediction of the types of problems that might be encountered during production.

One long standing battle has been against the crystallization and deposition of paraffin before, during and after production. As early as 1868[1] paraffin deposits were reported to be hindering production, and in the 1920s oil companies complained of deposits fouling production tubing, lifting rods, and pumps.[2] Problems arising from paraffin deposition and its management currently cause losses of billions of dollars per year in the cost of chemicals, well shutdowns, equipment failure, extra horsepower requirements, and reduced production. As the

oil industry develops deep-water wells, wax mitigation and remediation costs will increase.

With such a large-scale problem, there has been a considerable effort to develop a universal method for retarding wax crystallization and deposition. The many techniques evaluated, and the few currently implemented, range from the use of mechanical tools to chemical treatments.[3] Mechanical methods involve physically cutting the paraffin by sending a scraper through the pipeline (pigging). Thermal techniques consist of reducing heat loss by insulating the pipeline or externally heating the system using steam or hot oil. Chemical treatments include use of solvents for dissolving paraffin and injection of wax crystal modifiers that depress the wax formation potential or alter the crystal morphology.[4] However, there is not a single, universally effective treatment because each reservoir is unique and typically requires a custom management program. Bos and vanden Haak[5] have suggested that for a treatment system to be effective it must inhibit or modify the growth of paraffin crystals.

In the 1980s, during the height of this search for reliable and affordable wax management methods, magnetic

fluid conditioners (MFCs) became widely available to the industry. According to John Corney, inventor and founder of one of the many magnetic tool suppliers, "By directing crude oil and water through a strong, permanent magnetic field, the growth pattern of paraffin and scale crystals is altered, inhibiting the build up of solids in the well and production equipment."[6,p.2] A system operating in accordance with Corney's claim which fulfills the guideline given by Bos and vanden Haak and is, therefore, worthy of serious consideration for treatment of paraffin problems. That the influence of passive magnetic fields should be those claimed by Corney and others is not obvious nor has clear scientific evidence been presented in support.

The focus of this research was to 1) develop a bench-top pipeline for monitoring wax deposition from liquids in a dynamic system; 2) provide the first controlled, reproducible experimental data on the influence of magnetic conditioning as a means of wax remediation. A novel instrument was developed to monitor simultaneously two identical flowing fluids; identical except for exposure of one of them to magnetic fields. Experimentally, the flow rates of two pipelines were monitored as the temperature of

a small section of each pipeline was decreased. The onset of wax deposition in the cooled section was noted by a concomitant marked change in flow rate. Examination of thermal flow profiles (temperature vs. flow rate) provided insight into the effect of MFCs on the temperature at which wax separates from the liquid phase. In addition, an instrument was developed for the deposition of treated and untreated paraffin on nickel and Teflon surfaces. The relative physical hardness of these solids was studied using a scratch test.

CHAPTER 2
PARRAFINIC CRUDES

Characteristics of Paraffinic Crudes

Crude oil is a complex system that can contain a variety of compounds, including paraffin wax. Paraffin wax is comprised of a wide range of high molecular weight hydrocarbons that are soluble at reservoir conditions. During production, temperature and pressure changes decrease the solubility of paraffin in the crude, and wax can begin to crystallize and eventually adhere to the surfaces of production equipment.

As previously mentioned, paraffin deposits have created production problems since the mid-1800s. Various methods have been developed for harvesting waxy crude from readily accessible wells. Presently a broad effort is under way to understand more about paraffin drop out and develop cost-effective treatments suitable for use in remote locations, including deep water. In support of this effort, experiments have been done to study the crystal

structures and other physical properties of paraffin wax, with emphasis on the study of crystal morphology, temperature effects, deposition mechanisms and composition of deposits.

Crystal Morphology

Early studies of the structures of paraffin crystals were undertaken in order to develop ideal methods for refining paraffin wax from crude oil; however, this was no simple task due to the polymorphism common in large paraffins. Consequently, controversy arose over the exact structure of paraffin solids, and those disagreements persisted for many years.

In 1926, Padgett *et al.*[7] reported the formation of two types of crystals: 1) plates; 2) needles. His microscopic studies showed the formation of thin plate crystals during slow cooling, from which needle-like crystals would grow. Buchler and Graves[8] reported that straight-chain paraffins (n-paraffins) crystallized as plates, along with an "impurity" they called "soft wax" that tended to crystallize as needles. Rhodes *et al.*[9] suggested a new mechanism in which wax crystallization was always initiated by the formation of plates. Rapid cooling of the system

would cause the plates to begin to curl on the edges and form a needle-like tube. In 1932 Katz stated that plate formation was required for needles to form and he considered needles to be comprised of several layers of plates.[10]

An in-depth study of paraffin crystallization by Ferris and Cowles[11] suggested the formation of needles from cyclic hydrocarbons and that branched-chain paraffin formed "mal-formed crystals." Clarke studied 23 types of pure hydrocarbon crystals and identified the factors which determine the formation of plates, mal-formed crystals, and needles, these were 1) the cooling rate; 2) the difference between the melting point of the pure hydrocarbon and crystallization temperature of the solution.[12] However, Edwards stated that wax did not tend to crystallize in any particular form, although plates were the most common.[13]

From this lengthy argument over crystal structures, the industry has presently come to an agreement. Paraffin crystals are considered to consist of straight chain, branched, and cyclic hydrocarbons in the range of C_{15} up to C_{80}, typically forming an orthorhombic lattice.[14] However, changes in the composition of the wax, and the physical conditions, can result in the formation of both

orthorhombic and hexagonal close-packed lattices. The paraffin crystals can form thin plates, needles or mal-crystals, with needles being the most problematic, as they often tend to form a compact, three-dimensional network.[4] In addition, plates can network after curling to form hollow needle-like tubes.

Temperature Effects

The temperature at which wax crystallizes is called the "cloud point" or Wax Appearance Temperature (WAT). Early methods determined the WAT using pressure cells with visual windows through which a sample could be examined under a microscope as the temperature of the cell was slowly decreased. The first appearance of wax crystals was noted by a marked change in the turbidity of the solution. Essentially the solution became cloudy, thus the term "cloud point". With time, the methods employed for WAT determination have become less subjective. Techniques include polarized microscopy, cold finger deposition of paraffin, differential scanning calorimetry, infrared detection/light scattering, viscometry, measurement of volume and density changes, and acoustic resonance.

Although the established techniques are many, no single technique is ideal in all applications, nor do the

results between them always agree. For instance, using three techniques--viscometry, polarized microscopy, and differential scanning calorimetry--to study a single system, Hamoruda and Viken[15] reported WATs of 32°C, 30.4°C and 20.5°C respectively. Clearly, the determination of the cloud point is not an exact science, and this is partially due to the complex nature of paraffinic crudes. A typical sample of crude can contain a broad distribution of paraffins. The higher molecular weight hydrocarbons, such as C_{50}, are less soluble and will crystallize at a higher temperature than a C_{18} paraffin. Depending upon the technique used, the cloud point measurement can be the result of the crystallization of either high or low molecular weight paraffins. Nevertheless, cloud point data does provide some helpful information for designing a production protocol. Generally, engineers determine the cloud point using several different techniques and, to be on the safe side, use the highest observed value in their design.

Below the cloud point, the presence of wax crystals can cause an additional problem by increasing the viscosity of crude oil. As more wax crystallizes, they can agglomerate, resulting in the formation of a viscous slurry

in the bulk of the oil. In pipelines operated at high flow rates this slurry decreases production due to greater resistance to flow, but does not stop production. However, in a system operated at low flow rates, the slurry may increase the viscosity so high as to stop the flow. The most drastic effect can occur in a static system. When the temperature of the bulk fluid drops below the cloud point, the agglomeration of wax crystals can form a complex network throughout the bulk. When this occurs, the oil becomes extremely viscous, like a gel. The gelled oil is difficult to pump and can prevent flow from being restored. The temperature at which the fluid gels is called the "pour point".

Wax Deposition

Wax deposition does not necessarily occur at the cloud point, but can occur upon surfaces cooler than the cloud point, such as pipe walls and production equipment. Complete blockage of pipelines is rare, but wax deposits do adversely effect production due to increased flow resistance, which increases horsepower requirements for pumping and reduces total throughput. To develop adequate

remediation methods, a sound understanding of the mechanism and composition of wax deposition is helpful.

Wax deposition tendency. Wax deposition tendency is a measure of the amount of wax that can be deposited in a given time period, for a given temperature range and flow rate.[16] A combination of techniques can be used to model wax deposition. Using a static cell cold finger for wax deposition allows the temperature regime and heat fluxes of a pipeline to be duplicated, but the system is static and does not account for the effects of flow. Flow loops can duplicate the flow rates of a pipeline, but matching the heat flux is difficult. Tube blockage rigs are used to monitor the pressure drop across a cooled small-bore capillary caused by wax deposition. This technique is used to determine the rate of wax deposition and to evaluate the effectiveness of chemical wax inhibitors.

Deposition variables. Wax can adhere to any surface cooler than the WAT of the crude. The rate of wax deposition is directly controlled by several factors: the temperature of the bulk crude and pipe wall; viscosity; and the flow rate. The rate of wax deposition is greatest if the temperature of the bulk is just below the cloud point and the pipe wall is much cooler than the cloud point. As

the bulk oil continues to cool, the viscosity increases, hindering the migration of the wax from the bulk to the pipe surface. The rate of wax deposition reaches a minimum as the temperature of the bulk approaches the ambient temperature. In laminar flow systems, the wax deposition rate is highest, with the deposits being soft. As the flow rate increases the wax deposition rate decreases and the deposits become harder as soft structures in the wax slough off in the flow while the more durable ones accumulate on the walls.

Wax Remediation Tactics

Because of its potential adverse effects in oil production, a considerable effort has been made to develop techniques to manage wax-laden fluids. Some tactics seek to prevent the formation of wax crystals or alter the crystal structure, while others focus on methods to remove wax deposits. The techniques evaluated, and currently implemented, range from mechanical to chemical treatments.[3]

Mechanical techniques require direct access to the pipeline. The most common technique is the use of a scraping device called a "pig", which is launched into the pipeline and carried along by the flow. The shape of pigs

depends upon their design, but the pig's main function is to scrape wax deposits from the walls of a pipeline and push them ahead to an accessible collection station. "Pigging" is a routine maintenance for transmission pipelines with paraffin problems. Pigging is effective, but can cause problems if the pigs become lodged in the production equipment. This method is not usually used in oil wells themselves, as there is generally no way to launch a pig at the bottom of the well. Well maintenance often requires pulling the pump and rods and cutting the accumulated wax with special knives. Another mechanical method is the use of coiled-tubing used to flush wax from a pipeline with a high-pressure fluid.

By keeping the temperature of the bulk fluid above the cloud point, wax crystallization and deposition can be inhibited. This is typically accomplished by insulating the pipeline from the environment. The use of vacuum insulated tubing, bundled flowlines, and "pipe-in-pipe" configurations have been employed successfully. Hot-oiling a well involves flushing a well with oil that has been heated well above the cloud point of the crude. The hot oil melts wax deposits and removes the paraffin from the well.

Chemical treatments are used to prevent the formation of or modify the structure of wax crystals. Chemical treatments are seldom ideal and must be custom designed for each well. A novel chemical treatment introduces into the fluid flow two chemicals that react exothermically, raising the temperature of the crude significantly to melt any wax deposits. However, the reaction used generates a large quantity of nitrogen gas, sometimes increasing the pressure of the pipeline to hazardous levels.

More recently, novel techniques have been tested and are currently being evaluated. Pipe coatings, such as ceramics and Teflon, have been used, but with little success. Phillips Petroleum evaluated the effectiveness of 39 different coatings.[16] In some cases, wax deposition rates actually increased for certain coatings. In addition, most coatings are not robust and fail quickly. Other techniques, which have had little success, include using acoustic waves to remove wax and applying electrical impulses to "crack" long-chain paraffins into smaller hydrocarbons. A different approach, which if it works, would be elegant for its simplicity, and remarkable for its non-obviousness, involves the use of magnets to control wax in crude oil. This is the method addressed in this work.

Magnetic Fluid Conditioners

Magnetic fluid conditioners (MFCs) are reportedly the long awaited universal wax remediation devices; at least according to the MFC vendors. As previously stated, MFC vendors claim that "by directing crude oil and water through a strong, permanent magnetic field, the growth pattern of paraffin and scale crystals is altered, inhibiting the build up of solids in the well and production equipment."[6,p.2] However, such claims have been made without the support of sound scientific data.

The application of MFCs for treating scale deposits in water systems has been extensively field tested with varied results. Most of the claims of success are anecdotal testimonies and not based upon scientifically verifiable principles. For example, Szostak[17] reported that using a magnetic conditioner in their cooling towers resulted in cleaner heat exchangers that required less frequent cleaning. Similar claims have been made for MFCs used in the petroleum industry for the reduction or complete elimination of paraffin deposits.

The design of MFCs varies from vendor to vendor. Some vendors claim that conditioners that use permanent magnets are useless, while others argue that only permanent magnets

will provide the desired effect. Some "tools" clamp on the outside of the pipe, while others are designed to be placed within the pipeline. Some vendors state that MFCs must be designed according to specific parameters, such as exposure time and flow rates; as a result, they believe that studies of the effects of magnetic conditioning in the laboratory are meaningless because of the difficulty in duplicating exact pipeline conditions. However, if the claims that MFCs prevent wax deposition by altering the crystal structure of paraffin are true, then some evidence of the effect should be obtainable in the laboratory.

The anecdotal testimonies are not reason enough to support the application of MFCs in the oil field, but as the claims are so widespread, an investigation of their accuracy is called for. If magnetic conditioners are effective, they could provide a non-invasive, cost-effective means for retarding wax deposition in oil wells, pipelines, and deep-sea tiebacks. The goal of this research was to evaluate the effectiveness of magnetic conditioners, and determine the effect, if any, on the wax deposition temperature and the physical characteristic of deposits.

CHAPTER 3
EXPERIMENTAL

To achieve the principal goal of the experiment required the development of a pipeline to monitor two flows simultaneously, identical except for their exposure to magnetic fields. For the two individual flows to be identical, careful attention to the construction of two identical pipelines was critical. To guarantee consistency in the sample composition and flow rates, both pipelines need to be supplied by a single sample source. A cooling stage was incorporated to facilitate the deposition of paraffin within a localized zone. In addition, flow rates had to be measured precisely and compared. No commercial recording flow meters were found which would operate reliably at the flow rates required for this experiment. It was, therefore, necessary to design and fabricate novel flow meters for this use. These were placed in the flows, downstream of the cooling and isothermal stage. Finally, to facilitate investigations of the physical characteristics of wax deposits, a wax deposition stage was

included at the terminus of the pipeline. The following discussion outlines the details of the design and construction of the pipeline, thermal stages, flow meters, and wax deposition stage.

Pipeline

The pipeline was constructed from 304 stainless steel tubing ranging from 1/4 - 1/16 inch outside diameter (O.D.). Section A, as shown in Figure 3-1, leads from the bottom of the sample cell and was constructed from 1/4 inch O.D. tubing, approximately 36 inches long. A special filter, described later, was placed in-line in this section to remove solids from the fluid. Beyond the filter, a 1/4 valve was included to isolate the test sections during sample loading.

Section B was composed of two sides, each with five segments of 1/8 inch O.D., 0.075 inch I.D. stainless steel tubing, machined to the required specifications. Segments B1 and B2, leading from the 1/4 inch tee-valve, were each 2.00 inches in length and attached to two-way, normally closed, 300-psi solenoid valves. The solenoid valves permitted the divided flows to be stopped individually. Extending from the solenoid valves to the first elbows were

segments B3 and B4, 3.00 inches in length. Segments B1 - B4 allowed the two sides of the pipeline to be isolated so that either segment B5 or B6 could be exposed to a magnetic field without exposing the other side.

Some magnetic conditioning vendors claim that their devices utilize the Lorentz effect of force on an electrical charge q moving normal to the direction of magnetic induction, B. This force, $\vec{F}=q\vec{B}\times\vec{v}$, where $\vec{v}$ is the relative velocity of the charge in the field, is quite low for ionic species under typical flow conditions. It was necessary to design the experiment to investigate this effect in the laboratory, but the small samples of crude oil available and the elected protocol that the oil would not be recirculated, as in a loop for example, precluded using high flow rates to generate significant Lorentz forces. The chosen design overcame this restriction by setting the magnets into motion to obtain a large relative velocity. To achieve this, segments B5 and B6, 24 inches in length, were fabricated with a U-shaped loop to accommodate the moving magnetic conditioner (Figure 3-2). The specifics of all magnetic conditioners used will be discussed later. Segments B7 and B8 were machined to a

length of 6.75 inches and segments B9 and B10 to 6.00 inches. Segments B9 and B10 terminated section B at 1/8 - 1/16 inch stainless steel reducers.

A cooling stage, an isothermal stage, and digital flow meters comprised section C. The pipeline reduced from 1/8 inch O.D. tubing to 1/16 inch O.D., 0.030 inch I.D. stainless steel, capillary tubing at the cooling stage. In the laminar flow regime the flow rate is proportional to the fourth power of the radius of the pipe. Deposition of the slightest amount of wax on the walls of small I.D. tubing would result in a significant change in the radius of the pipe and consequently a marked change in the flow rate. Therefore, using 0.030 inch I.D. tubing enhanced the sensitivity of the flow measurements.

From the cooling stage, the pipeline returned to 1/8 inch O.D. tubing through the isothermal stage and terminated beyond the flow detectors. Two 24-inch sections of 1/8 inch O.D. 0.075 inch I.D. rubber tubing were attached to the outlet of the flow detectors and the inlet of the wax deposition stage.

At the midpoint of the project, modifications were made in the flow lines to accommodate test of a commercial magnetic conditioner. Two 48-inch attachments, shown in

Figure 3-3, were connected to the pipeline, at the junctions of segment B5-B7 and B6-B8, via 12-inch lengths of 1/8 inch stainless steel tubing. Each attachment consisted of a 72 inch, U-shaped length of 1/8 inch stainless steel tubing encased in 1/2 inch PVC pipe through which a 50% ethylene glycol and 50% water mixture from a constant temperature bath was circulated.

Filter

The dead crude oil samples studied were unfiltered and typically contained small amounts of solids which could have easily plugged the fine capillary tubing. To prevent such a problem, a unique filter was designed and incorporated into section A of the pipeline. The filter was comprised of three components: 1) a filter housing; 2) an end cap; 3) a wire mesh screen.

The filter housing was designed to hold an air conditioner filter from a 1983 Buick. The housing, and end cap, were machined from 304 stainless steel according to the specifications given in Figure 3-4 and Figure 3-5 respectively. An assembly drawing is shown in Figure 3-6.

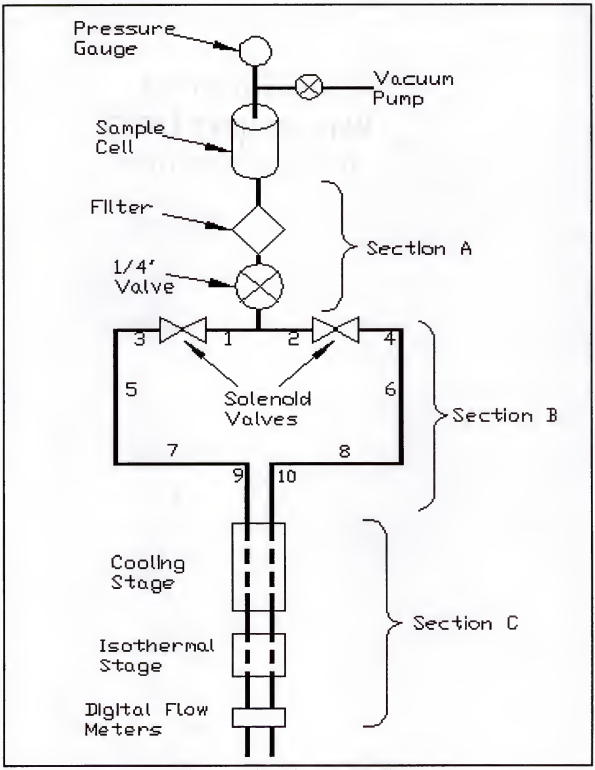


Figure 3-1: Schematic of pipeline assembly.

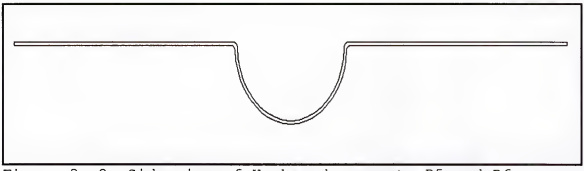


Figure 3 -2: Side view of U-shaped segments B5 and B6.

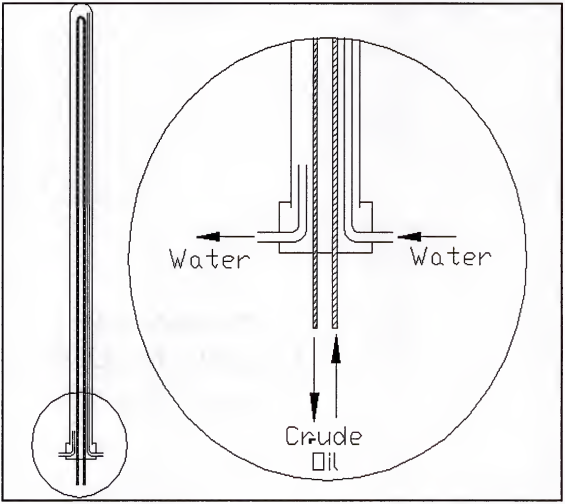


Figure 3-3: Schematic of attachments to section B to incorporate a commercial magnetic conditioner.

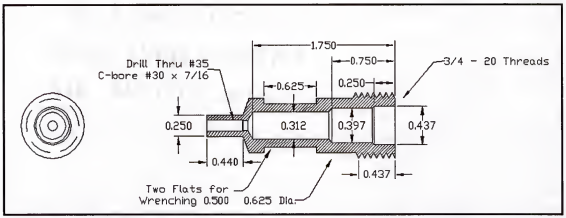


Figure 3-4: Top and side view of stainless steel oil filter housing.

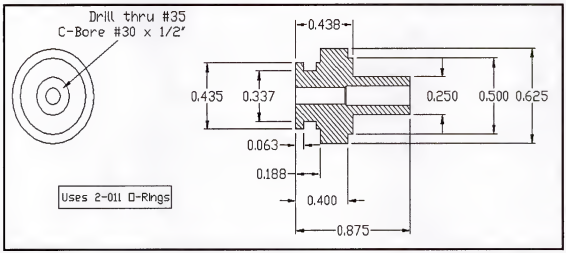


Figure 3-5: Top and side view of stainless steel cap.

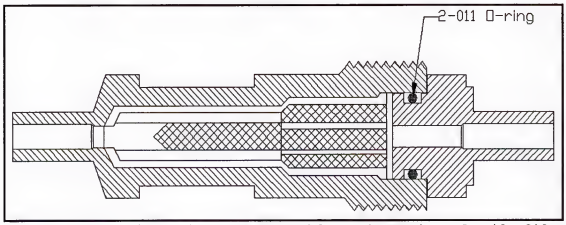


Figure 3-6: Side view of assembly schematic of oil filter housing.

Cooling Stage

The cooling stage was designed to allow the temperature of two 8.00 inch sections of 1/16 inch stainless steel, capillary tubing to be varied over ranges appropriate for deposition of wax from the oil to be studied. These were from 10°C to 80°C. Peltier heat pump devices were used to promote heat flow between the capillaries and an isothermal block maintained at a fixed temperature by flow of a mixture of 50% ethylene glycol and 50% water, chilled to 5°C and circulated through 3/8 inch copper tubing.

To insure the stage reached thermal equilibrium quickly, copper was chosen as the construction material because of its high thermal conductivity. Two plates were machined to 8.00 inches by 2.37 inches from 1/4 inch copper, as shown in Figure 3-7. Twenty-one 0.191 inch clearance holes were drilled through each plate. Two 9-inch lengths of 1/16 inch, 304 stainless steel, capillary tubing were soldered to plate A 0.500 inch apart on center. An platinum resistance temperature device (R.T.D.) mount was machined from brass and soldered to plate A near the middle of the plate on the centerline. A 12-inch, U-shaped

section of 3/8 inch copper tubing was soldered to plate B. The 3/8 inch tubing was used for circulating the chilled ethylene glycol/water mixture.

Before assembling, the bottom sides of plate A and B were covered with a thin film of thermocouple compound to promote good thermal contact. Four Peltier junctions were placed between the two plates, which were secured using 10-32 nylon screws and nuts, as shown in Figure 3-8. Nylon screws were used in order to insulate the copper plates from each other, electrically and thermally.

Isothermal Stage

The isothermal stage construction is similarly to the cooling stage. The isothermal stage plates were machined from 1/4 inch copper to 4.00 inches by 2.37 inches. A pattern of eleven 0.191 inch clearance holes was drilled through each plate, as shown in Figure 3-9. On plate A, two six-inch lengths of 1/8 inch 304 stainless steel tubing were soldered 0.500 inch apart, on center. An R.T.D. mount, identical to the one used on the cooling stage, was soldered near the middle of plate A on the centerline. Two peltier junctions were used as the heating source and the chilled ethylene glycol and water mixture was used as the

cooling source. The inside surfaces of both plates were covered with a thermocouple compound and the stage assembled using 10-32 nylon screws and nuts, as shown in Figure 3-10.

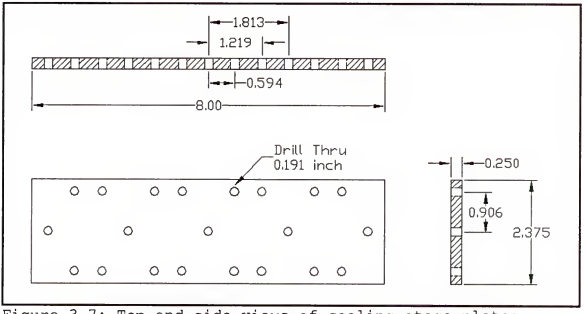


Figure 3-7: Top and side views of cooling stage plates.

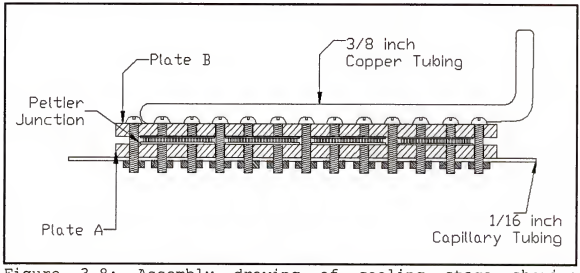


Figure 3-8: Assembly drawing of cooling stage showing Peltier junctions, capillary and copper tubing.

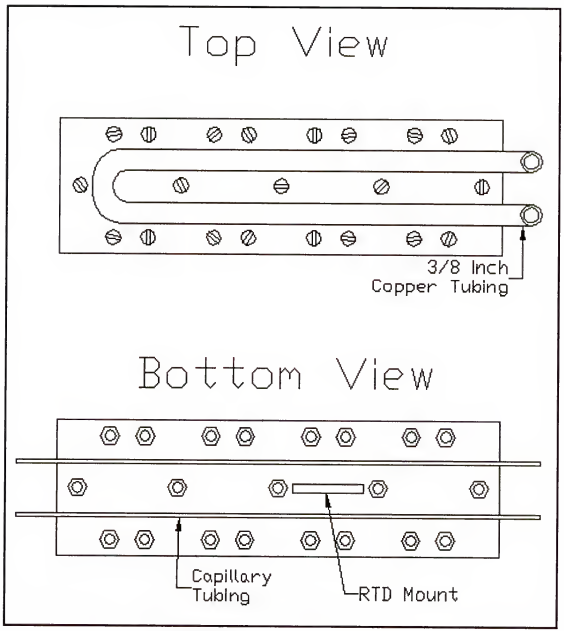


Figure 3-9: Assembly drawing of cooling stage; top and bottom views.

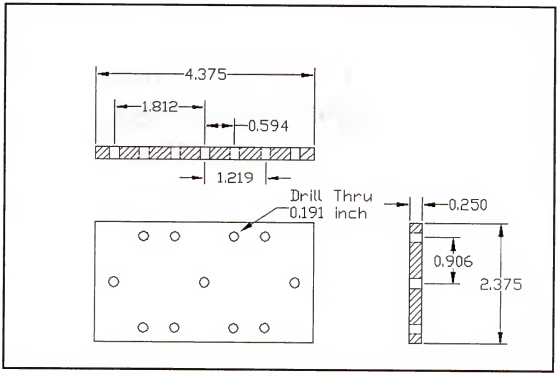


Figure 3-10: Top and side views of isothermal stage plates.

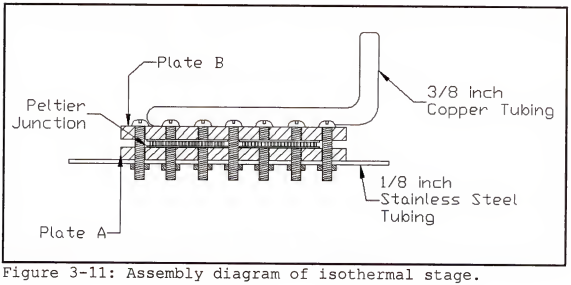


Figure 3-11: Assembly diagram of isothermal stage.

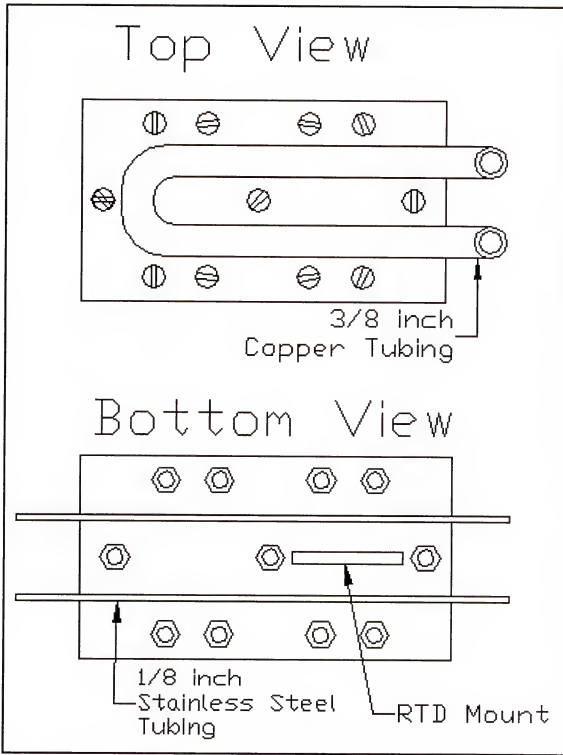


Figure 3-12: Assembly drawing of isothermal stage; top and bottom views.

Digital Flow Meters

Crude oil can behave as either a Newtonian or non-Newtonian fluid, depending upon the temperature and the composition of the fluid. Above the cloud point, the viscosity of the crude oil is largely a function of the temperature, a characteristic of most Newtonian fluids.[18] However, as the temperature drops below the cloud point and paraffin begins to crystallize within the bulk fluid, the viscosity of the fluid becomes a function of both the temperature and the shear rate (non-Newtonian fluid). The change in the viscosity as the crude oil transitions from a Newtonian to a non-Newtonian fluid can be seen in a plot of the natural logarithm of the viscosity versus temperature, as shown in Figure 3-13.[16] Note the rapid increase of the viscosity between 40°C and 30°C. This deviation from linearity is the point of transition from a Newtonian to non-Newtonian fluid.

In the laminar flow regime, the flow rate is inversely proportional to changes in the viscosity of a liquid; therefore, an increase in the viscosity of the fluid would be noted by a decrease in the flow rate. If a sample transitioned from a Newtonian to a non-Newtonian fluid, then the drastic change in the viscosity would result in a

significant change in the flow rate. However, the flow rate is also directly proportional to the fourth power of the radius of the pipe. If wax deposition occurs on the walls of a small radius pipe, such as capillary tubing, the resultant change in the flow rate would be significantly greater than the change due to an increase of the viscosity.

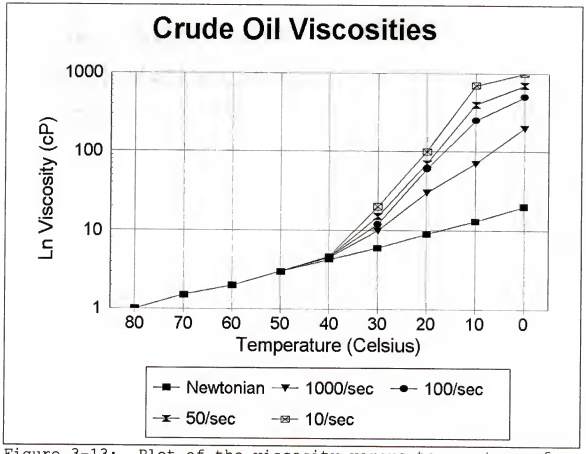


Figure 3-13: Plot of the viscosity versus temperature of a waxy crude.

To be effective, the digital flow meters used for this experiment had to be sensitive enough to differentiate

between a change in the flow rate due to wax deposition and a change due to a Newtonian/non-Newtonian transition. An adequate flow meter would be robust, highly sensitive to the slightest changes in the flow rate and able to respond quickly. A set of detectors was designed and built to fulfill these requirements.

Each detector consisted of two glass-encapsulated thermistors, one used as a reference and the other as the sensor. Thermistors typically have an accuracy of ±0.02 °C and can detect temperature changes as small as 10^{-3} °C.[19] The thermistors were arranged in a Wheatstone bridge configuration, as shown in Figure 3-14. In the bridge, a resistor, R2, balances R1, a calibrated variable resistor. One of the thermistors, attached to the isothermal stage, functions as the reference resistance, R_3, for the bridge and the other thermistor, R_4, placed within the fluid flow, functions as the sensor.

As current flows through the bridge, the thermistors are heated. If the bridge is balanced, $IR_1 = IR_2$ and $IR_3 = IR_4$, then there is no current flow from a to b. However, as the fluid flows over the sensor, some of the i^2R Joule heat will be removed from the thermistors, increasing the

resistance at R_4. The change in R_4 resistance unbalances the bridge, resulting in a current flow from a to b. The greater the flow rate, the greater the difference between R_3 and R_4, and the higher the current across the bridge.

For this experiment, Mr. Steve Miles of the departmental electronics shop designed a circuit incorporating the bridge outlined above. The flow rates were measured as a function of voltage. A detailed schematic of the flow meter circuit is shown in Appendix A.

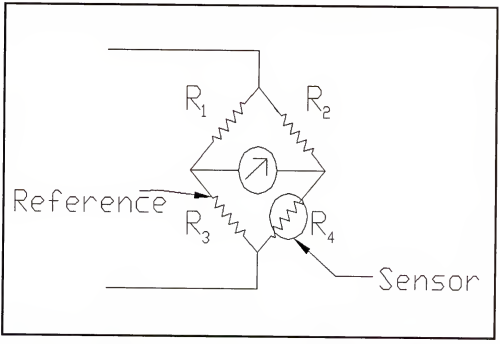


Figure 3-14:Schematic of bridge circuit for digital flow meters.

Wax Deposition Stage

Analysis of the effects of a magnetic field on the physical properties of the wax complemented the flow measurements. The problem was obtaining the wax samples. Collecting samples of wax directly from the small bore pipeline was not practical, so an alternative method was developed. Samples of wax were obtained by deposition on nickel and Teflon surfaces by cooling the two streams of paraffinic crude below the wax deposition temperature. Three plates comprised the wax deposition stage: an aluminum top plate, a Teflon plate to serve as a seal, and a stainless steel trough along with several peripheral parts. The entire assembly was attached to an aluminum heat sink with a Peltier junction placed between a brass inlay and the heat sink. The Peltier junction was the cooling source for the stage.

Stainless Steel Trough

The bottom plate was machined from 0.250 inch, 304 stainless steel. A 1.628 inch by 0.1875 inch deep notch was machined in the middle of the stainless steel plate, and a 1.625 inch by 1.625 inch by 0.1873 inch thick inlay of brass was brazed in place prior to machining the trough.

The stainless steel/brass trough was machined to a length of 8.750 inches by 1.625 inches wide, as shown in Figure 3-15. The 0.125 inch wide by 0.100 inch deep grooves provided troughs for the two streams of oil to flow down and over nickel foil strips. In the center of the plate, the 0.375 inch counter-bore was drilled to accommodate a temperature probe.

Teflon Plate and Aluminum Top Plate

The Teflon and aluminum top plates were used to seal the troughs and prevent cross contamination of the two fluid flows. Each plate was machined to 8.00 inches by 1.625 inches. The Teflon plate was machined from a 0.125 Teflon sheet and the top plate from 0.250 inch aluminum. Identical hole patterns were drilled in each plate, as shown in Figure 3-16.

Peripheral Parts

Peripheral parts were designed to deliver the sample flows from the pipeline and to hold the nickel strips in place. The parts were machined according to the specifications given in Figures 3-17 and 3-18. All of the parts were machined from brass except for part 3-18b, which

was machined from 304 stainless steel. The assembly of parts 3-18a-d allowed the tension of the nickel strips to be adjusted. Part 3-17 clamped the nickel strips in place and delivered the sample fluids to the troughs. An assembly drawing of the wax deposition stage is shown in Figure 3-19. When assembled, the deposition stage provided two identical rectangular conduits for the two oil flows. The lower surface of each conduit was deep chilled to promote precipitation of heavy hydrocarbons from the oil.

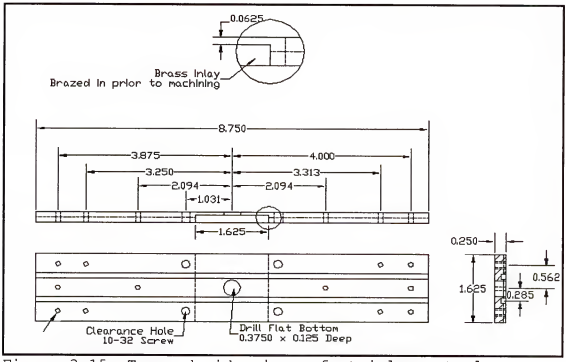


Figure 3-15: Top and side views of stainless steel trough

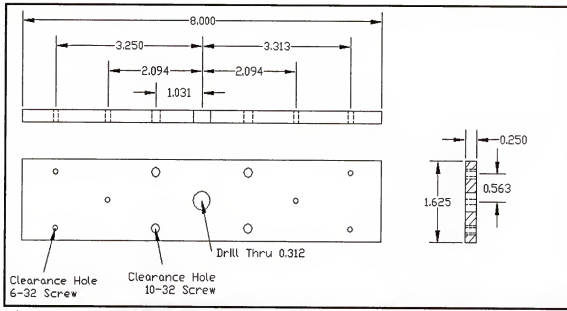


Figure 3-16: Top and side views of Teflon and aluminum plates.

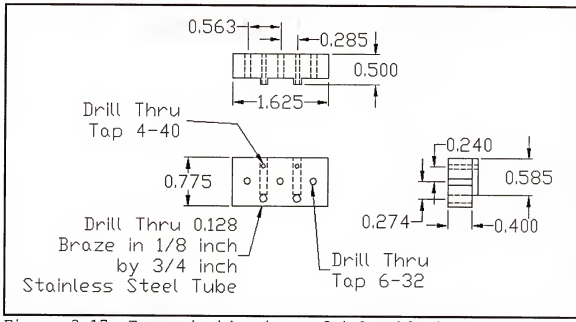


Figure 3-17: Top and side views of inlet block

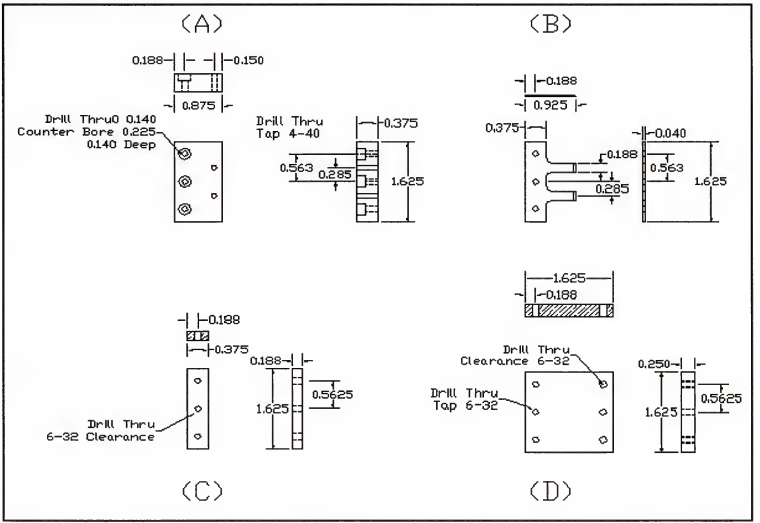


Figure 3-18: Top and side views of peripheral parts of wax deposition stage.

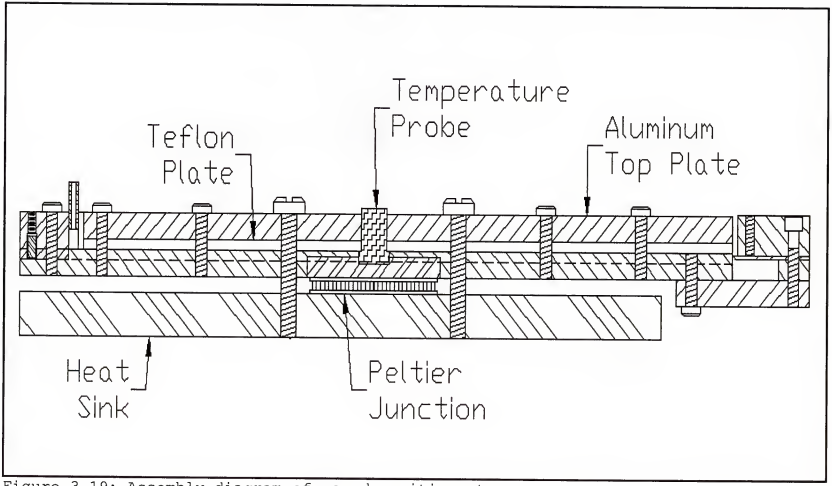


Figure 3-19: Assembly diagram of wax deposition stage.

Magnetic Fluid Conditioners

Magnetic fluid conditioners are devices which are used to expose flowing fluids to a magnetic field. The debate over the effectiveness of permanent magnets versus electromagnets is ongoing; therefore, both types of magnets were used for this experiment. Tests were performed using permanent magnets arranged in several different orientations in addition to a commercial magnetic conditioner.

The first magnets used were rare earth, permanent magnets (approximately 800 gauss) arranged on a disk such that the magnetic field was perpendicular to the direction of flow. As previously mentioned, some of the magnetic conditioner vendors claim that their devices utilize the Lorentz effect of force on an electrical charge moving normal to the direction of magnetic induction, B. To obtain a high relative velocity between the fluid and the magnet, the magnets were placed into motion by attaching the disk to a motor. Figure 3-20 shows the design of this magnetic conditioner, hereafter referred to as conditioner UF1. After assembly, the disk was placed in either of U-shaped sections, B5 or B6, of the pipeline.

The "wheel" was attached to a motor and operated at 3000 RPM.

A second conditioner, UF2, was evaluated using sets of permanent magnets, arranged so that the magnetic field was oriented perpendicular to the fluid flow. The magnets were clamped onto the exterior of segment B5 and B6. A third magnetic conditioner tested was a commercial electromagnet, Para-Mag, provided by George Fourqurean of Solar Injections, Incorporated. In this device, the magnetic field is oriented parallel to the fluid flow. The specifics of the Para-Mag design are proprietary and will not be discussed here.

Finally, a fourth conditioner, UF3, consisting of a pair of permanent rare earth magnets, polarized to facilitate an arrangement with the field directed parallel to the direction of flow was used. The magnets used for this configuration were attached to a stage, as shown in Figure 3-21, to allow the gap to be adjusted in order to vary the strength of the field.

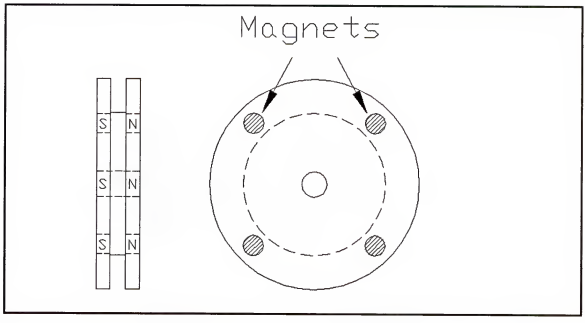


Figure 3-20: UF1 magnetic conditioner.

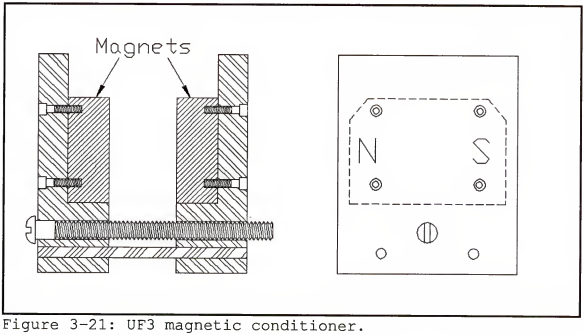


Figure 3-21: UF3 magnetic conditioner.

Oil Samples

Crude oil samples obtained from several different wells were provided by oil companies which were members of the sponsoring consortium, DeepStar. Table 3-1 lists the samples by company name. The samples are considered to be "dead crude" due to the loss of light end gases.

Table 3-1: List of Dead crude oil samples.

Company Name	Oil Well	Sampling Point
Elf Exploration	Wellhead A-15	Main Pass 30
Elf Exploration	Wellhead A-4	Main Pass 293-A
Bristol Resources	Wellhead CL&F #1	Bayou Penchant
Giddings Austin Chalk	Johnnie Lee Kubecka #1	
Murphy Oil	Wellhead 068 #3	Ship Shoal Blk 118-R
Chevron	Well C-3	Main Pass 299C
Andarako Minerals	Wellhead 4225334134	Railroad Unit

Measurement Hardware and Interfacing

The temperature of the stages was measured using two-wire platinum resistance temperature devices (RTD), which were connected to Keithley model K-196 digital multimeters to obtain resistance values. The resistance values were later converted to the corresponding temperature using the following equation,

$$Temp = ((R - 100.0685)/(0.0039076*100.0685)),$$

where R is the resistance of interest. The specifics of the temperature control of the cooling and isothermal stage are discussed in Appendix B.

Glass encapsulated thermistors were used as the sensors for the digital flow meters, in conjunction with the circuit designed by Mr. Miles. The voltage outputs of the circuit were linked to Keithley K-196 multimeters. The solenoid valves were connected to solid state relays which were actuated by a 3 volt output from a program controlled digital to analog converter board (Keithley model DAC-02).

All of the electronic components were linked to a micro-computer containing an Intel Pentium processor operating at 166 MHz with 32 megabytes of RAM. The multimeters were connected to the micro-computer using the standardized IEEE general purpose interface bus (GPIB), including the 8-bit i/o card and the required software.

Figure 3-22 depicts a schematic of the setup. A summary of the electronic equipment used is given in Table 3-2. Temperature and flow data were acquired using computer programs written specifically for this experiment by the author and Dr. Evan House. These programs were written using ANSI C standard code language and are listed in Appendix C.

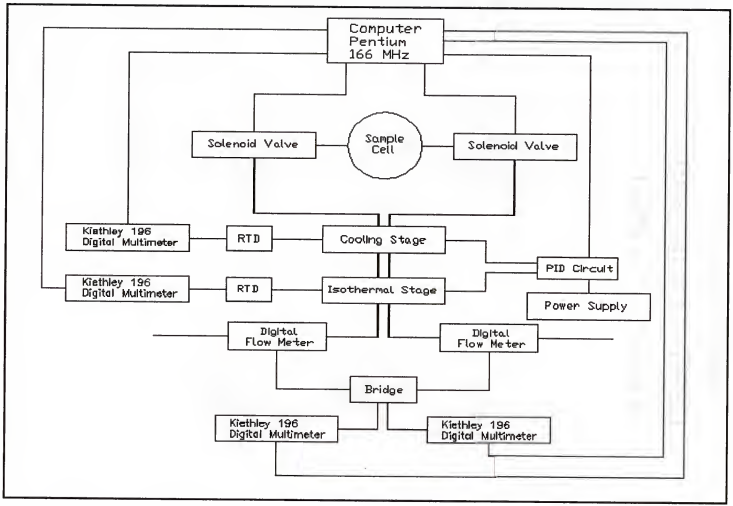


Figure 3-22: Schematic diagram of the electronic hardware setup.

Table 3-2 : Summary of measurement hardware.

Item	Manufacturer	Model Number	Range of Operation	Resolution (manufacturer's values)	Function
Digital Multimeter	Keithley Instruments Inc.	K196	20mV to 1000V; 20Ω to 20 MΩ, 2 to 4-terminal resistance measurements	Range dependent, see manual for details.	Measures voltage or resistance from temperature probes or flow meters.
Thermistor	DigiKey Inc.				Measures temperature in resistance
RTD	Omega Engineering Inc.	1PT100K2015	-200 to 750 °C	± 0.1% Ohms.	Measures temperature in resistance.

CHAPTER 4
EXPERIMENTAL PROCEDURE

Pipeline Assembly and Thermal Flow Data Acquisition

Initially, all components of the pipeline were carefully cleaned with soap and water, thoroughly rinsed with distilled water, followed by multiple washings of pentane and finally acetone. All components were baked at 70°C. The pipeline was assembled by connecting the 1/8-inch stainless steel sections using stainless steel Swage-Lok fittings. The pipeline was connected to the cooling stage with a 1/8 - 1/16 inch Swage-Lok reducer. Using 1/4-inch tubing, the sample cell was connected to the backing gas supply tank and a vacuum pump. The sample cell, pipeline, and ancillary components up to the cooling stage were enclosed within an oven that was controlled at 55°C, well above the wax deposition temperature (W.D.T.) of the crude oil samples.

Before loading, each crude oil sample was reconstituted by stirring and heating the sample above 60°C

for at least two hours. The sample cell was loaded by applying a vacuum to the cell. Once the sample cell was loaded, the oil was allowed to equilibrate overnight.

The PID controller was turned on with an initial set point of 40°C or the cooling stage, well above the WDT of the samples. The reference stage set point was 50°C throughout the entire experiment. Using 99.98% pure argon as the backing gas, the sample cell was pressurized and the solenoid valves opened to establish a steady state flow through both pipelines. The pressure of the argon was adjusted until the flow rate was between three and five cubic centimeters per minute.

While monitoring the flow rate of each side of the pipeline, the temperature of the cooling stage was decreased by one-degree steps. At each step of the cooling, the flow rate of each line and the temperature of the cooling were recorded. The temperature sweep continued until a marked change in flow rate of each pipeline was noted.

When wax deposition occurred in both lines, the solenoid valves were closed and the stage was quickly warmed to 40°C and allowed to reach equilibrium. The flow was reestablished and the procedure repeated.

Magnetic Conditioning Procedure

Analysis of the effectiveness of magnetic conditioners as a means of retarding wax deposition was carried out by exposing one branch of the pipeline to a magnetic field while isolating the other branch. The general procedure for obtaining thermal flow data was followed. Any effects due to the magnetic field were noted by a difference in the wax deposition behavior of the two branches. Variations in the WDT due to magnetic field exposure should be detectable on both sides of the pipeline; therefore, after exposing one side of the pipeline to a magnetic field, the magnetic conditioner was moved to the other side of the pipeline and the procedure repeated. Following this procedure, each magnetic conditioner was tested. Only effects which reproducibly appear always in the exposed branch and which do not occur when the magnets are omitted are considered as positive.

Wax Deposition Procedure and Hardness Testing

Before assembling the wax deposition stage, each part was thoroughly cleaned with acetone and allowed to air dry. 1/8 inch wide Nickel ribbons, 12 inches in length, were cleaned using acetone and placed in each trough of the

stage. To insure good thermal contact between the deposition stage and the nickel strips, one end of each strip was secured, the strips were pulled taut and the other end secured. The assembled stage was attached to the pipeline using 1/8 inch tubing.

The temperature of the wax deposition stage was controlled at 0°C using a Peltier plate and DC power supply. After each trial, the nickel strips and the Teflon plate were removed from the stage and examined to determine the extent of wax deposition. The Teflon plate and the nickel strips were rinsed with methyl ethyl ketone to remove oil residues and other solids. The hardness of the remaining wax deposits was evaluated using a scratch test.

To perform the scratch test, the Teflon surface, or Nickel strip, was secured to an aluminum plate, which was clamped to the table of a milling machine. The device used for the scratch test, shown in Figure 4-1, was mounted in a drill chuck so that the pin was touching the surface of the Teflon. The milling table was raised 0.010 of an inch and moved longitudinally so that the pin moved across both wax deposits. This step was repeated, raising the table before each attempt, until a scratch appeared in either, or both,

of the surfaces. Each sample was tested this way several times.

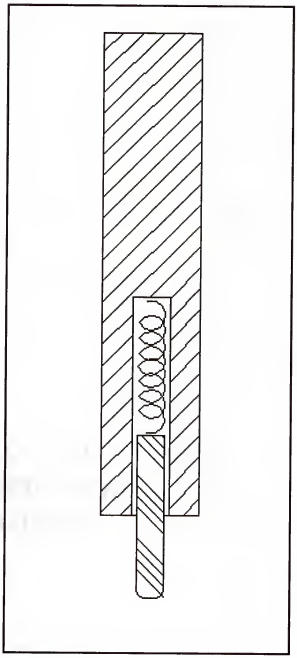


Figure 4-1: Side view of device used for scratch test.

CHAPTER 5
RESULTS

Analysis of thermal flow data for evidence of wax deposition provided initial confirmation of the new apparatus and technique for the determination of the wax deposition temperature. Wax deposition was noted by a marked change in the flow rate, which can be seen in a plot of the flow rate parameter versus the fluid temperature, in addition to the accumulation of wax on the surfaces of the wax deposition stage downstream of the capillary tubing. Wax deposition behavior within the capillary tubing of the cooling stage section was dependent upon the cooling rate of the stage and the flow rate of the system. Preliminary experiments revealed what ranges of these variables were appropriate for these tests.

If the flow rate was too fast, the onset of wax formation would not be highly resolved. If the flow rate was too fast, the liquid would not reach equilibrium with the stage and wax crystals might not form at all. After several trials, with different samples, a suitable cooling rate appeared to be about one degree Celsius per four

minutes, at a flow rate of three to five cubic centimeters per minute. Subsequent data were collected at or near these settings.

Proof of the effectiveness of the apparatus was followed by evaluation of the effects of magnetic conditioning on the WDT. Therefore, the following data and plots will be discussed in two groups: 1) data obtained before magnetic conditioning; 2) data obtained while one side of the pipeline was magnetically conditioned.

Thermal Flow Profiles Before Magnetic Conditioning

Thermal flow data was collected for each of the seven samples. Figures 5-1 through 5-7 depict representative thermal flow profiles for each sample. Table 5-1 lists the samples tested, the figure number of the corresponding thermal flow profile, and whether or not wax accumulation on the deposition stage occurred.

Magnetic Conditioning Data

A variety of magnetic conditioners was evaluated. The bulk of the data were collected for samples which showed strong evidence of wax deposition. Table 5-2 lists the

samples used, their corresponding figure numbers, and the conditioner used. Figures 5-8 through 5-13 depict representative thermal flow profiles of magnetically conditioned samples.

Wax Hardness Analysis

The wax deposition stage provided three cooled surfaces to facilitate wax deposition: the stainless steel stage; the nickel ribbons; the Teflon surface. Surprisingly, the wax generally deposited preferentially on the Teflon. Deposits on the nickel surface tended to be soft, containing a considerable amount of occluded liquid. Attempts to wash away the latent oil from the nickel ribbons resulted in removing the wax also, while the deposits on the Teflon were quite tenacious. The wax hardness of the deposits on the Teflon surface was evaluated using the "scratch" test. In every case, no significant difference in the hardness of wax deposits was noted.

Table 5-1: List of Crude samples, the corresponding Figure number and whether or not wax accumulation was seen.

Name of Sample	Corresponding Figure Number	Wax Accumulation downstream?
Elf Exploration Well A-4	Figure 5-1	YES
Elf Exploration Well A-15	Figure 5-2	YES
Bayou Penchant	Figure 5-3	NO
Giddings Austin Chalk	Figure 5-4	NO
Murphy Oil	Figure 5-5	NO
Chevron Well C-3	Figure 5-6	NO
Andarako Minerals	Figure 5-7	YES

Table 5-2: List of conditioned samples and their corresponding figures.

Name of Sample	Corresponding Figure number	Magnetic Conditioner
Andarako Minerals	5-8 & 5-9	Para-Mag
	5-12	UF3
Elf Well A-4	5-10	Para-Mag
	5-15	UF2
Elf Well A-15	5-11	Para-Mag
	5-13	UF3
	5-14	UF1

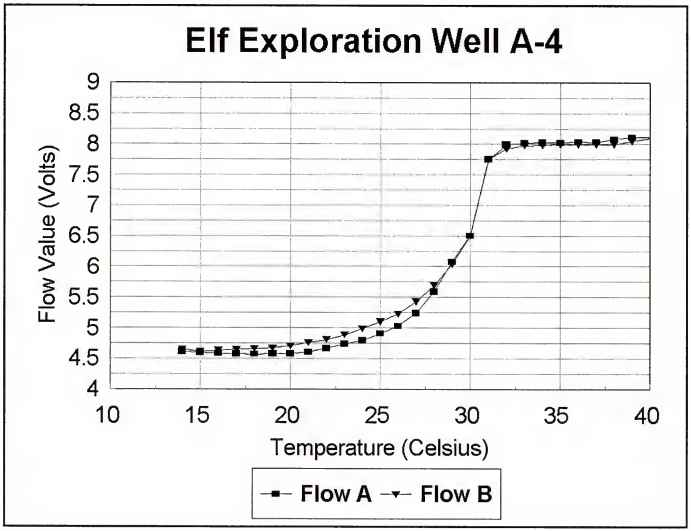


Figure 5-1: Representative thermal flow profile of Elf Exploration well A-4 sample without magnetic conditioning.

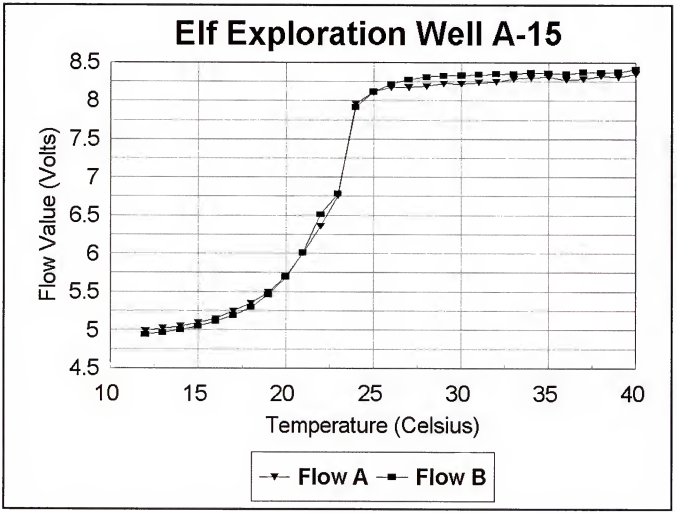


Figure 5-2: Representative thermal flow profile of Elf Exploration well A-15 sample without magnetic conditioning.

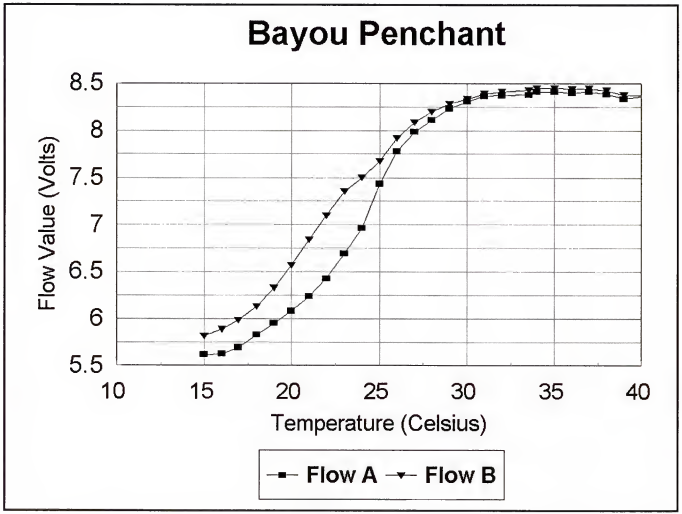


Figure 5-3: Representative thermal flow profile of Bayou Penchant sample without magnetic conditioning.

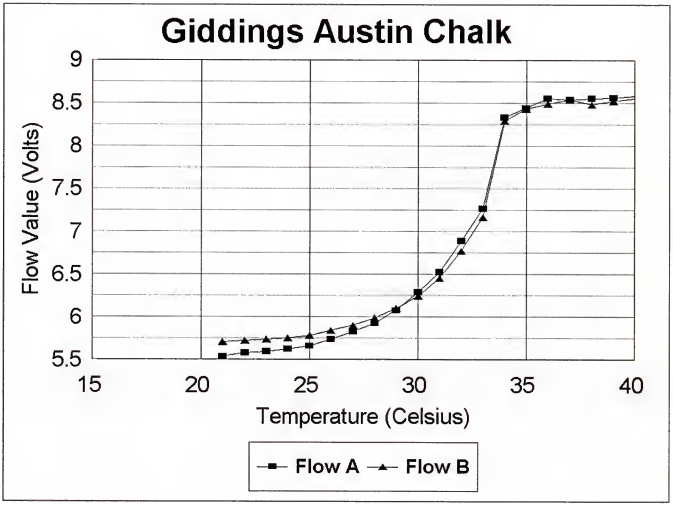


Figure 5-4: Representative thermal flow profile of Giddings Austin Chalk sample without magnetic conditioning.

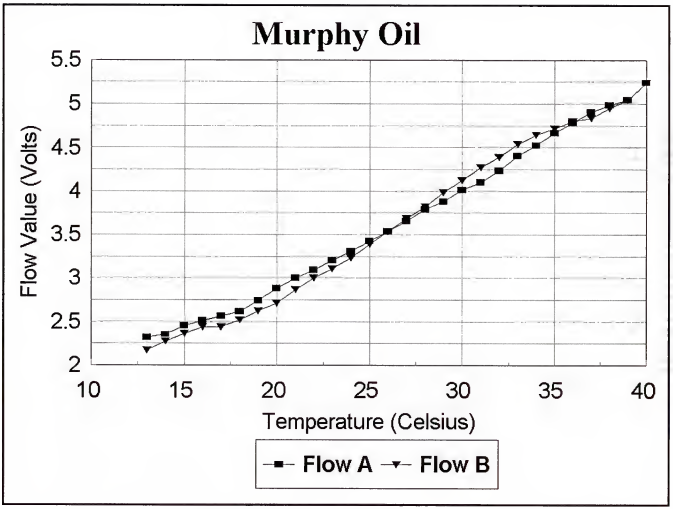


Figure 5-5: Representative thermal flow profile of Murphy Oil sample without magnetic conditioning.

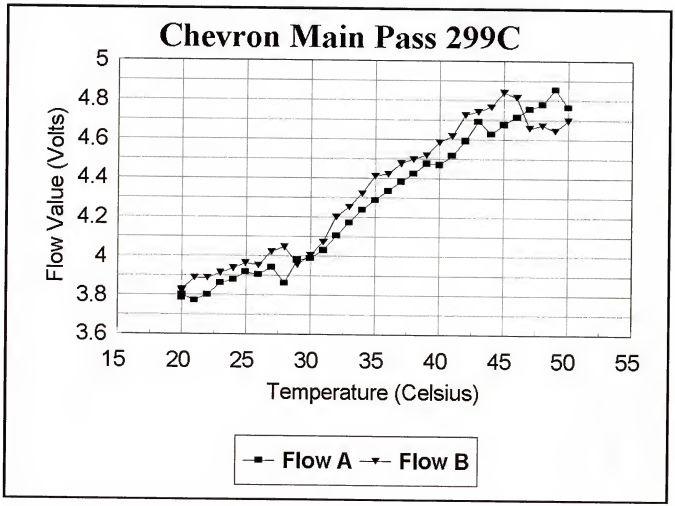


Figure 5-6: Representative thermal flow profile of Chevron Well C-3 sample without magnetic conditioning.

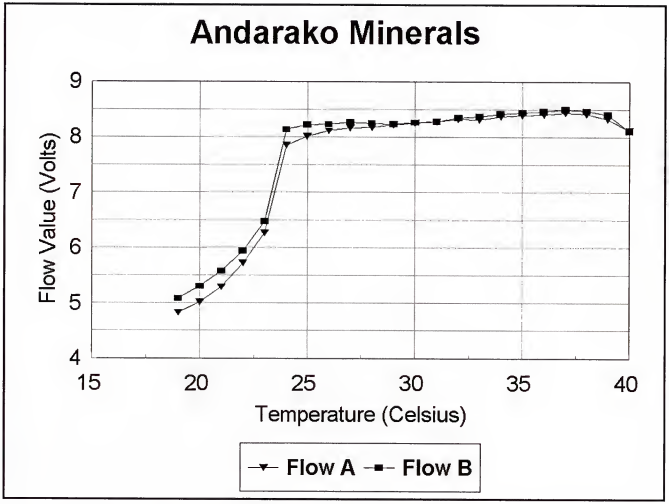


Figure 5-7: Representative thermal flow profile of Andarako Minerals sample without magnetic conditioning.

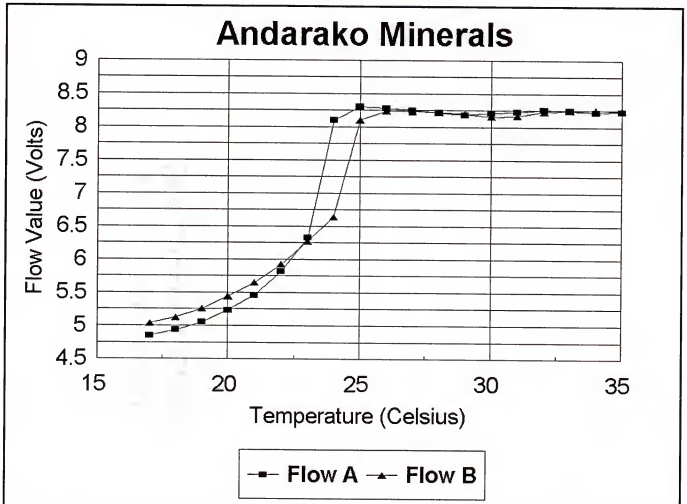


Figure 5-8: Representative thermal flow profile of Andarako Minerals sample. Flow A was conditioned by the Para-Mag device.

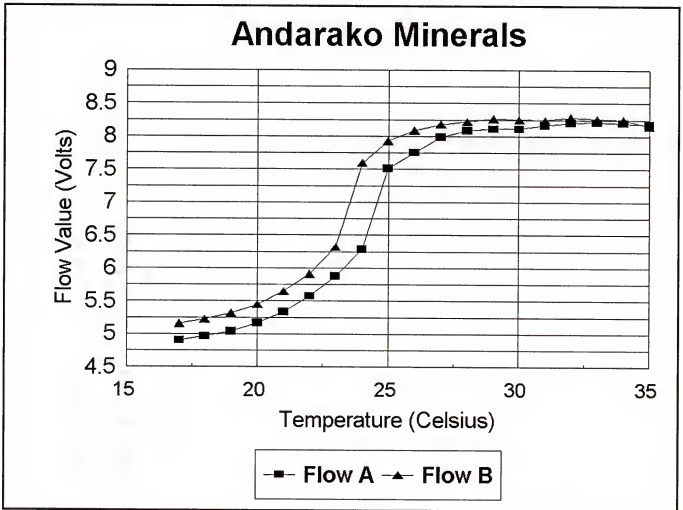


Figure 5-9: Representative thermal flow profile of Andarako Minerals sample. Flow B was conditioned by the Para-Mag device.

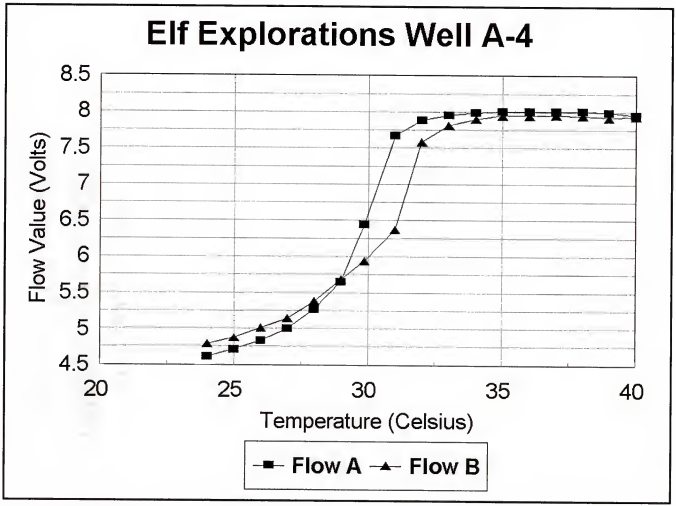


Figure 5-10: Representative thermal flow profile of Elf Exploration well A-4 sample. Flow A was conditioned by the Para-Mag device.

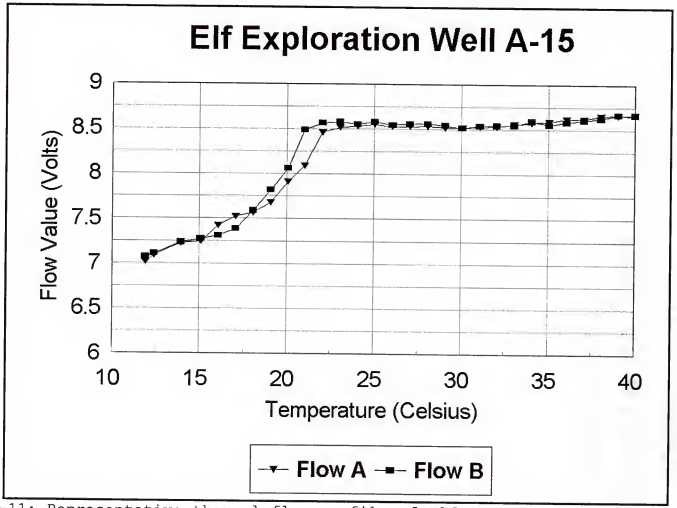


Figure 5-11: Representative thermal flow profile of Elf Exploration well A-15 sample. Flow B was conditioned by the Para-Mag device.

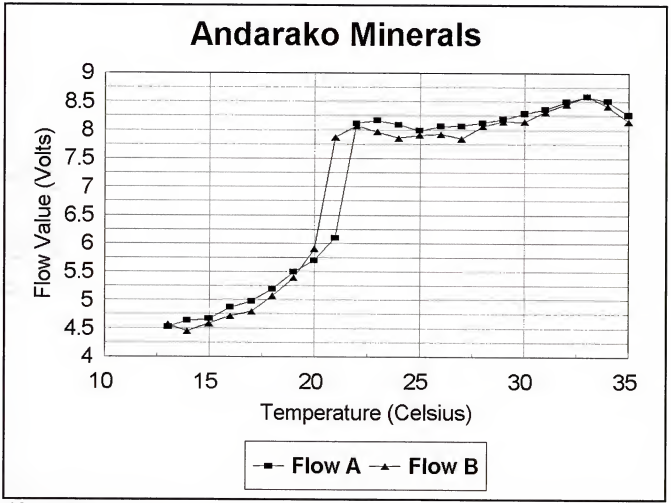


Figure 5-12: Representative thermal flow profile of Andarako Minerals sample. Flow B was conditioned by the UF3 conditioner.

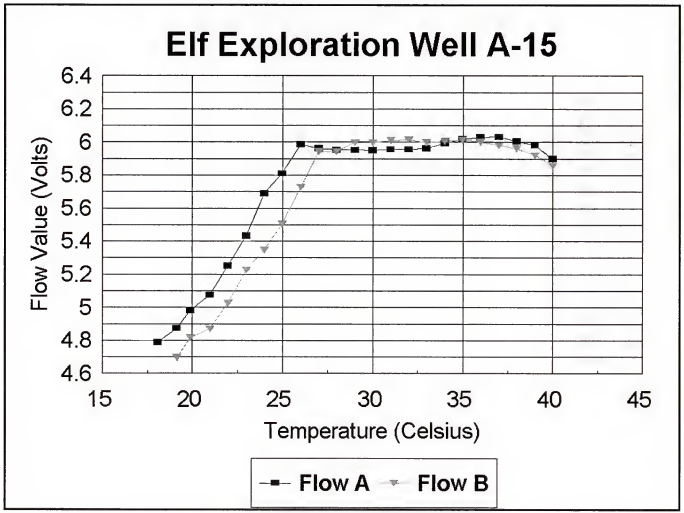


Figure 5-13: Representative thermal flow profile of Elf Exploration well A-15. Flow A was conditioned by the UF3 conditioner.

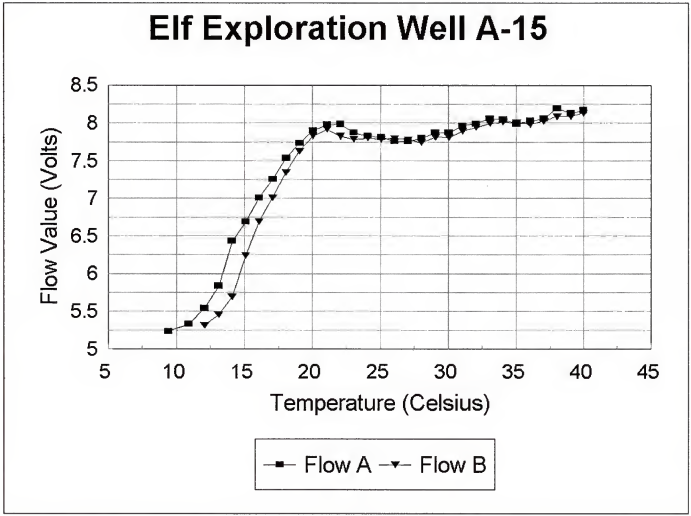


Figure 5-14: Representative thermal flow profile of Elf Exploration well A-15 sample. Flow A was conditioned by the UF1 conditioner.

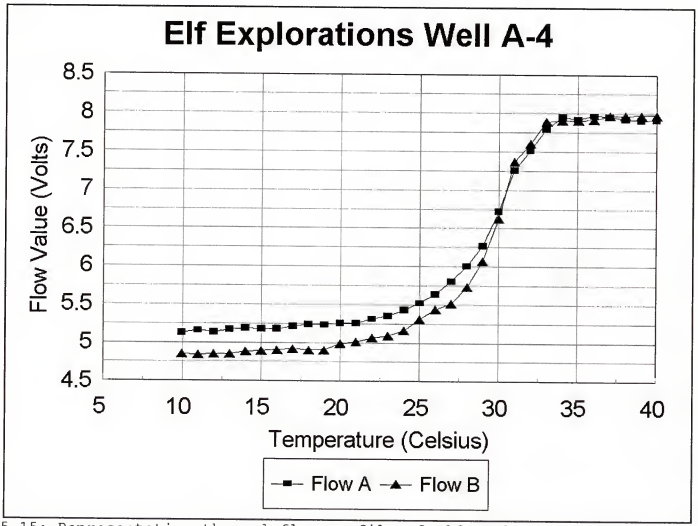


Figure 5-15: Representative thermal flow profile of Elf Exploration well A-4 sample. Flow A was conditioned by the UF2 conditioner.

CHAPTER 6
DISCUSSION AND CONCLUSION

The research reported here had a twofold focus: 1) to build an apparatus for monitoring wax deposition from liquids in a dynamic system; 2) provide the first controlled, reproducible, experimental data on the influence, if any, of magnetic conditioning on wax deposition. An apparatus was designed, built and tested to accomplish the first goal and facilitate the evaluation of magnetic conditioners. In addition, several different magnetic conditioning devices were tested, and their effect on the WDT determined.

Sensitivity of Digital Flow Meters

Figures 5-1 through 5-7, clearly depict the apparatus response to wax appearance in the cooling stage. The custom digital flow meters were sensitive enough to measure changes in the flow rate due to the crystallization or deposition of wax. Examining the flow profiles of the Murphy Oil, Bayou Penchant, and Elf Exploration Well A-4 data confirms the sensitivity of the flow meters.

The Murphy sample was quite light with roughly the consistency of diesel fuel and with no noticeable quantities of solid wax in the sample container at room temperature. The linear nature of Figure 5-5 suggests that wax deposition did not occur in trials using the Murphy Oil sample, and this was confirmed by a lack of wax accumulation on the surfaces of the wax deposition stage. The linear nature of the profile suggests that changes in the flow rate were due to increase viscosity of the cooled fluid. This is characteristic of some Newtonian fluids.

The Bayou Penchant sample also had the consistency of diesel fuel with no accumulation of solid wax in the sample container. However, unlike the Murphy Oil sample, wax crystallization did occur. Figure 5-3 depicts a marked change in the flow rate near 27°C, which might be construed as the onset of wax deposition; however, this is not the case. The data suggests a Newtonian behavior down to 27°C, at which point a transition from Newtonian to non-Newtonian behavior occurred. This is supported by the absence of wax accumulation on the surfaces of the wax deposition stage. However, the oil did form a gel-like phase in the deposition stage, suggesting the presence of paraffin crystals suspended within the bulk of the fluid. This gel

phase is characteristic of a crude oil nearing its pour point, at which point the fluid is typically considered to be non-Newtonian.

Examining the thermal flow profiles of the Elf Exploration Well A-4 sample provides final confirmation of the sensitivity of the flow meters. Figure 5-1 depicts a marked change in the flow rate at 29°C that is not the result of a Newtonian/non-Newtonian transition, but is due to the onset of wax deposition. This was confirmed by the accumulation of wax on the nickel and Teflon surfaces of the wax deposition stage. Comparison of the Elf Exploration profile to the Bayou Penchant profile reveals that wax deposition is noted by a significantly greater change in the flow rate than the change due to the Newtonian/non-Newtonian transition.

Clearly, the digital flow meters fulfilled the requirements for which they were designed: To facilitate the determination of the WDT of crude oil. The flow meters were robust, enough so that the sensors have yet to be replaced or repaired.

Possible Design Improvements

The data supports that this apparatus is adequate for studying small sample volumes under laminar flow

conditions. Information about the behavior of wax in the turbulent flow regime would be very useful. This apparatus, or a modified version of it, could be used for turbulent flow studies; however, such trials would require large sample volumes, which were not practical for this experiment. The use of larger sample volumes would permit the instrument design to be changed to incorporate the larger ID pipe required to achieve turbulent flow of crude oils. Another reason for selecting laminar flow was to avoid the further complication implicit in the high shear forces the oil would experience in the pumps necessary to produce fast flow. The molecular structure of the oil could be modified by these forces. Any fractionation of large molecules would diminish the wax drop out potential.

The current design does not permit the examination of the extent of wax deposition within the cooling stage section. An additional improvement would be the design of a cooling stage that incorporates larger ID tubing that could easily be removed. This would facilitate examination of the extent of wax deposition within the cooling stage. However, such an improvement might require the development of new flow meters.

The Effects of Magnetic Conditioning

The exposure of the flowing fluid to magnetic fields oriented perpendicular to the fluid flow did not have a noticeable effect on the WDT of the crude. However, this was not the case with the Para-Mag and UF3 devices. The use of a magnetic field parallel to the fluid flow appears to have an effect.

The Para-Mag device was the first unit in these experiments to exhibit an effect. A one-degree depression of the WDT is noticeable in Figure 5-8 for the conditioned section of the pipeline. To insure this effect was due to the magnetic field and not some artifact of the instrument, the Para-Mag unit was transferred to section B of the pipeline and additional data obtained. The same effect was exhibited, as shown in Figure 5-9. A comparison of several consecutive trials using the Para-Mag unit reinforced the legitimacy of this effect. Figures 6-1 and 6-2 depict combined plots of the conditioned and unconditioned data from four separate trials on a single sample. The effect is consistent from trial to trial. A similar effect was exhibited when additional samples were tested, as shown in Figures 5-10 and 5-11.

An additional concern was the heat dissipated by the electromagnet of the Para-Mag device (approximately 150 watts). Replacing the Para-Mag unit with a comparable, non-magnetic heat source and re-testing the samples verified that the WDT depression was not due to a heat effect (see Figure 6-3).

Thermal flow data of samples conditioned by the UF3 (permanent magnet) conditioner provided additional confirmation of the effect of a parallel magnetic field. Figures 5-12 and 5-13 show that the effect seen using the Para-Mag device is reproducible using permanent magnets. The variability of the gap between the magnets on the UF3 device facilitated studying the effects of varying the field strength. The magnetic field strength of the UF3 device was varied from 3000 to 500 gauss. From Figure 6-4, one can see that varying the field strength over this range did not have an effect on the WDT. These data suggest that the system might be saturated at low field strengths.

Additional research into the effects of magnetic conditioning can be carried out on a micro-scale level. Determination of whether or not the crystal structure is altered by a magnetic field would provide some valuable information. Further research should focus on the crystal

morphology and deposition mechanism of paraffin before and after magnetic conditioning.

A goal of this research was not to explain why magnetic conditioners work, but simply to show whether or not MFCs have any effect on the WDT. The work presented in this document suggests that ***some*** "magnetic fluid conditioners" have a ***small*** effect on the WDT of ***some*** crude oils. No work has yet been done to optimize this effect. Passing judgement as to the usefulness of magnetic conditioners to the petroleum industry, at this point, would be premature. Obviously, a one-degree depression of the WDT would be of little benefit. However, if further research were to determine the mechanism of this effect, then its magnitude could perhaps be magnified to a useful level. At any rate its cause remains to be explained, and clearly this work shows one place where new science and new understanding await discovery.

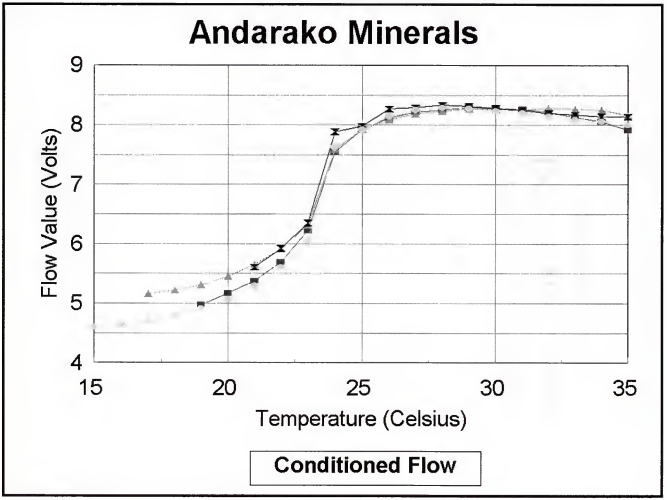


Figure 6-1: Combination of Para-Mag conditioned data from the Andarako Minerals trials.

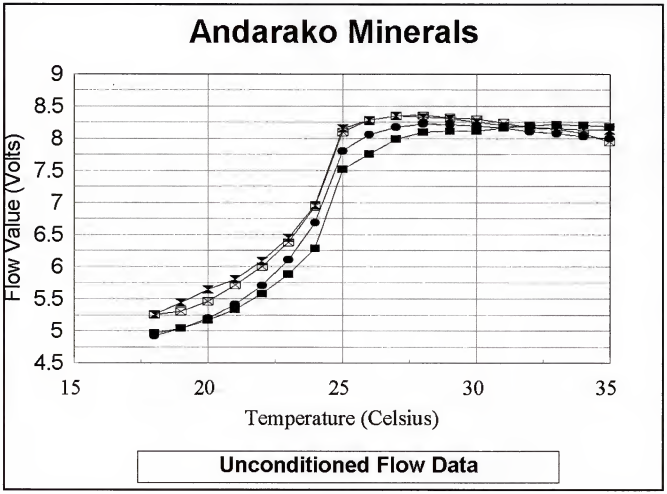


Figure 6-2: Combination of unconditioned data from the Andarako Minerals trials.

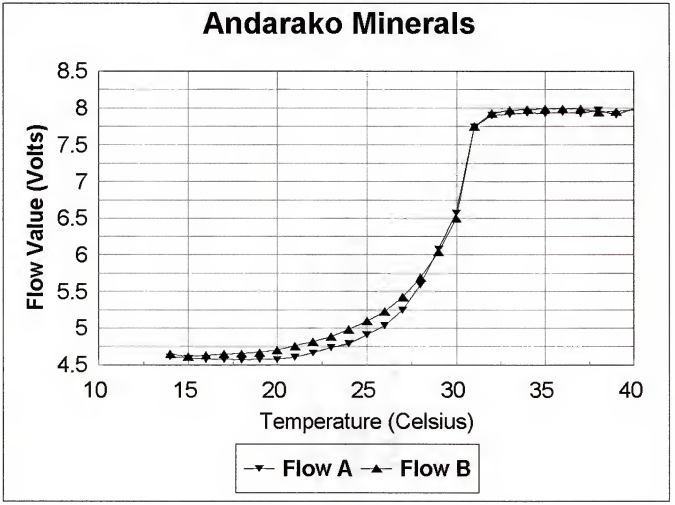


Figure 6-3: Thermal flow profile of Andarako Minerals sample with flow A conditioned by a non-magnetic heat source.

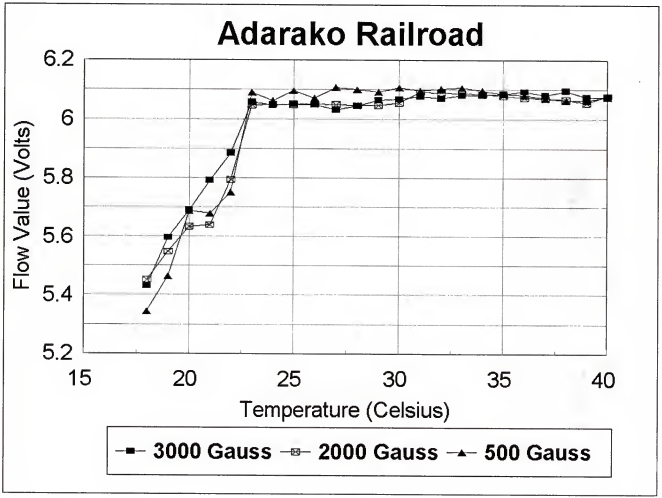


Figure 6-4: Andarako Minerals sample thermal flow profiles of data collected at various field strengths. The UF3 conditioner was used for these trials.

APPENDIX A
DIGITAL FLOW METER CIRCUIT

The schematic of the digital flow meter circuit, designed and fabricated by Mr. Steve Miles of UF, is shown in Figure A-1 on the following page.

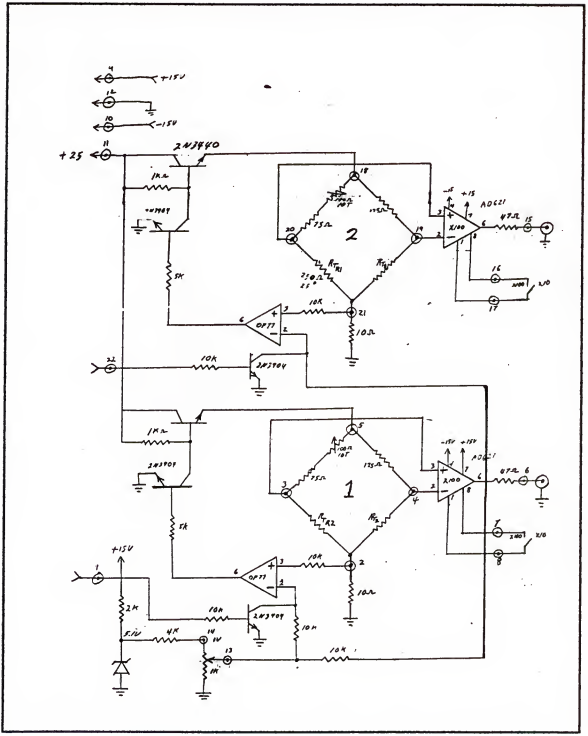


Figure A-1: Schematic of digital flow meter circuit.

APPENDIX B
TEMERATURE CONTROL

Accurate temperature control of the isothermal and cooling stage was required in order for the apparatus to be effective. The deposition of wax within the capillary tubing of the cooling section was possible because of the adequate control of the temperature during the cooling cycle. In addition, the accuracy of the flow meters was dependent upon precise control of the temperature of the isothermal stage.

Recall that each temperature stage consisted of several Peltier junctions sandwiched between two copper plates. Each stage was cooled by circulating a 50% water and 50% ethylene glycol solution through 3/8 inch copper tubing. The temperature of the water/glycol solution was controlled at 5°C. The Peltier junctions served as the heat source for the stages. Each stage was controlled at the desired setpoint by controlling the current flow through the Peltier junctions. This was made possible by the PID algorithm developed by Dr. Evan House, see Appendix

C, and the six Peltier control circuits, designed by Mr. Steve. Miles, see Figure B-1.

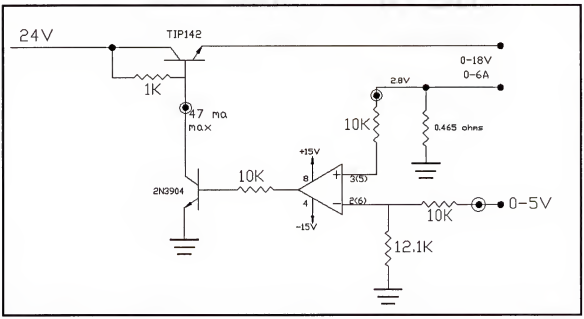


Figure B-1: Schematic of Peltier control circuit designed by Mr. Steve Miles.

To ensure that the temperature control was adequate, initial experiments were performed where the temperature of each stage was recorded as a function of time. Figure B-2 depicts the data from a cooling sweep in 1°C increments. The time required for temperature equilibration during a cooling cycle was approximately 3 minutes. Figure B-3 depicts the temperature of the isothermal stage versus time. The plot indicates the capability of controlling the temperature of the stage at 323.15K (50.00°C) with a standard deviation of ± 0.005K over the 2 hour time period.

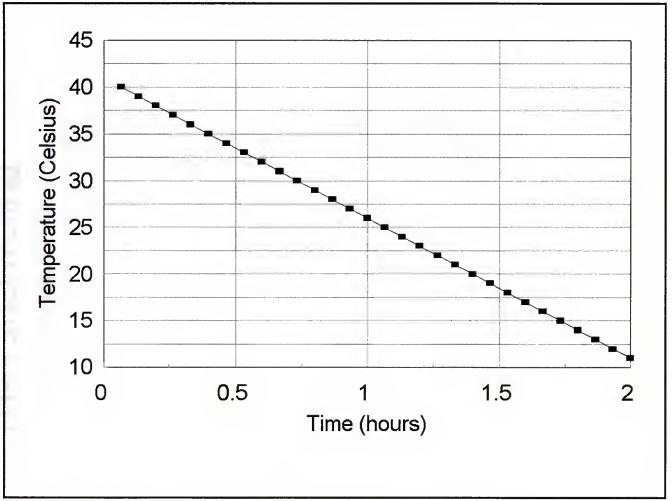


Figure B-2: Cooling stage temperature versus time plot of a system undergoing a programmed 1.0°C temperature change.

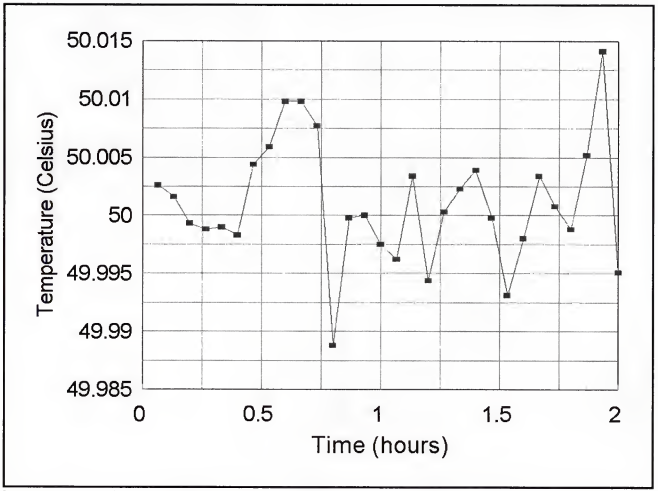


Figure B-3: Plot of isothermal stage temperature control over a period of 2 hours at a setpoint of 323.15K (50.00°C) with a standard deviation of ± 0.005K.

APPENDIX C
COMPUTER PROGRAM

The source code for the program used for the temperature control and data acquisition is listed below. The program was a cooperative work between the author and Dr. Evan House. The program was written using ANSI C standard code language.

```
#include <stdio.h>
□
#include <stdlib.h>
□
#include <math.h>
□
#include <string.h>
□
#include "DECL.H"                /* supplied with driver
libraries */
□
#include <conio.h>
□
#include <time.h>
□
#include <graph.h>
□

□

□
FILE *stream1, *stream2, *stream3;

#define CARDNUMBER     0x02e2
```

```
#define ICRO            0xd000
#define DAI             0x0000
#define IDNRO           0xc000
#define ADC             0x0009
#define AWCRO           0x1000
#define SHOB            0x0001
#define ARCRO           0x0000
#define DAAD            0x0000
#define AWRO            0x3000
double press_ac, press_out, press_e[2], press_pb,
press_der, press_inn,
       press_in[2], press_sp, press_band, press_mul,
press_pbmul,
       press_inmul,press_dermul, press, press_watch,
press_set_point;

double temp_ac, temp_out, temp_e[2], temp_pb, temp_der,
temp_inn, temp_in[2],
       temp_sp, temp_band, temp_mul, temp_pbmul,
temp_inmul, temp_dermul, temp, temp_set_point,
temp_sp_change;

double flow_a, flow_b, diff_flow;

float t[2], ttrip, sweep_period, sweep_step, press_sp1,
sweep_watch, num_steps;
int count_1, count_2, k;
char inchar;

void get_input_data(void);
void control_temp(void);
void control_press(void);
void output_data(void);
void setup_screen(void);
void change_temp_setpoint(void);
void reverse_sweep(void);
void graph_flow_diff(long number, double value, double
value1);
void findminmax(double *buffer2, double value, double
value1, double *Min1, double *Max1, double *Min, double
*Max);

double rdrtd(void);
double rdpress(void);
```

```
double rdflow_a(void);
double rdflow_b(void);
static double buffer[4096];
static double buffer1[4096];
static double buffer2[4096];
double graph_spec;



□
main()
□
{
□
  clock_t ticksnow;
□
  int  n, cycle;
□

□
  stream1 = fopen("c:\\mag\\data\\ptdat.out", "a");
  stream3 = fopen("c:\\mag\\data\\temp.out","a");

  outpw(0x370, 0<<4);              /* shifts registers */
  outpw(0x372, 0<<4);

  get_input_data();

  _displaycursor(_GCURSOROFF);
  _wrapon(_GWRAPOFF);
  _clearscreen(_GCLEARSCREEN);         /*Setup Display */
  _setvideomode(_VRES16COLOR);
  setup_screen();
  _settextwindow(3,39,25,60);

   t[0]=0.1f;
   ttrip=0;
   press_in[0]=0;
   temp_in[0]=0;
   press_watch=(press_sp)*150.3591+1.49;
   k=1;

  while(n!=1)
```

```
{
 ticksnow=clock();
 t[1]=((float)ticksnow/CLK_TCK);

 temp_ac=rdrtd();                /* READ RTDS */
 press_ac=rdpress();

          /* Convert RTD readings to Celcius */

 temp=((temp_ac-100.0685)/(0.0039076*100.0685));
 press=((press_ac-100.0685)/(0.0039076*100.0685));

 control_temp();
 control_press();

 flow_a=rdflow_a();            /* READ FLOW METERS */
 flow_b=rdflow_b();
 diff_flow=(flow_a-flow_b);


 _clearscreen(_GWINDOW);
 output_data();             /* Output Data to Screen */
 k++;
 graph_spec=.0500;
 graph_flow_diff(k, flow_a, flow_b);

t[0]=t[1];

if( kbhit())
{
inchar = (char)getch();
switch( inchar )
 {
   case 'p' :       /*Change Sweep Stage Setpoint*/
                    /*      by +1 degree         */

   case 'P' :

        temp_sp_change = temp_sp_change + 1;

        temp_sp = temp_sp_change;

        temp_sp = 100.0685*((0.0039076*temp_sp) + 1);
```

```
            break;

      case 'o' :       /*Change Sweep Stage Setpoint*/
      case 'O' :       /*      by -1 degree          */


            temp_sp_change = temp_sp_change - 1;

            temp_sp = temp_sp_change;

            temp_sp = 100.0685*((0.0039076*temp_sp) + 1);

            break;

      case 's' :      /* Begin Sweep */
      case 'S' :
           n=1;
           break;
      case 'a' :         /* Exit Application */
      case 'A' :
         outpw(0x370, 0<<4);
         outpw(0x372, 0<<4);
         exit(0);
         break;
      case 'q' :                          /* Open Valve */
      case 'Q' :
         outpw(0x372, 4095<<4);
         break;
      case 'z' :                          /* Open Valve */
      case 'Z' :
         outpw(0x370, 4095<<4);
         break;
      case 'w' :                          /* Close Valve */
      case 'W' :
         outpw(0x372, 0<<4);
         break;
      case 'x' :                          /* Close Valve */
      case 'X' :
         outpw(0x370, 0<<4);
         break;
   default : break;
     }
   }
```

```
    }

    n=1;
    count_1 = 1;

          /* Print Data to File Temp.out */

    fprintf(stream3, "%d    %.4f   %.4f   %.4f    %.4f
%.4f\n", n, press, temp, flow_a, flow_b, t[1]);

   change_temp_setpoint();   /*Change Sweep Setpoint*/

    ticksnow=clock();
    t[1]=((float)ticksnow/CLK_TCK);
    sweep_watch=t[1];


for(cycle=0; cycle<10; cycle++)
{

   do
   {
    if( kbhit())
    {
    inchar = (char)getch();
    switch( inchar )
     {
       case 'a' :                    /* Exit Application */
       case 'A' :
          outpw(0x370, 0<<4);
          outpw(0x372, 0<<4);
          exit(0);
          break;
       case 'q' :                     /* Open Valve */
       case 'Q' :
          outpw(0x372, 4095<<4);
          break;
       case 'z' :                     /* Open Valve */
       case 'Z' :
          outpw(0x370, 4095<<4);
          break;

       case 'w' :                     /* Close Valve */
```

```
        case 'W' :
           outpw(0x372, 0<<4);
           break;
        case 'x' :                      /* Close Valve */
        case 'X' :
           outpw(0x370, 0<<4);
           break;
        default : break;

      }
     }

     ticksnow=clock();
     t[1]=((float)ticksnow/CLK_TCK);

     if(t[1]>sweep_watch+(sweep_period*60))
      {

        n=n+1;
            /* Print Data to File Temp.out */
       fprintf(stream3, "%d    %.4f   %.4f   %.4f    %.4f
%.4f\n", n, press, temp, flow_a, flow_b, t[1]);

        change_temp_setpoint();

        sweep_watch=sweep_watch+(sweep_period*60);
      }

      temp_ac=rdrtd();                  /* READ RTDS */
      press_ac=rdpress();

      temp=((temp_ac-100.0685)/(0.0039076*100.0685));
      press=((press_ac-100.0685)/(0.0039076*100.0685));

      flow_a=rdflow_a();                /* READ FLOW METERS */
      flow_b=rdflow_b();
      diff_flow=(flow_a-flow_b);

      control_temp();
      control_press();

      _clearscreen(_GWINDOW);     /*Output Data to Screen */
      output_data();
```

```
    t[0]=t[1];
    }
while(n<((int)num_steps+1));

     n=1;

     reverse_sweep();

     change_temp_setpoint();
     ticksnow=clock();
     t[1]=((float)ticksnow/CLK_TCK);
     sweep_watch=t[1];
}

     outpw(CARDNUMBER+ICRO, DAI);
     outpw(CARDNUMBER+IDNRO, ADC);
     outpw(CARDNUMBER+AWCRO+SHOB, 0);
     outpw(CARDNUMBER+ARCRO, DAAD);
     outpw(CARDNUMBER+AWRO, 0);

     outpw(CARDNUMBER+ICRO, DAI);
     outpw(CARDNUMBER+IDNRO, ADC);
     outpw(CARDNUMBER+AWCRO+SHOB, 1);
     outpw(CARDNUMBER+ARCRO, DAAD);
     outpw(CARDNUMBER+AWRO, 1);


    fclose(stream1);                /* Close Data Files */
    fclose(stream3);

    _setvideomode(_DEFAULTMODE);
    return(0);
}



         /*****************************************/
         /* Retrieve Setup Data for P.I.D. Control  */
         /* Integration, derivative, etc. variables */
         /* From Sweep.dat file.                    */
         /*****************************************/

void get_input_data(void)
{
```

```
float temp_band1, temp_inmul1, temp_dermul1,
      temp_pbmul1, temp_sp1;

float press_band1, press_inmul1, press_dermul1,
      press_pbmul1;

stream2 = fopen("c:\\sweep.dat", "rt");

       fscanf(stream2, "%f/n",&num_steps);
       fscanf(stream2, "%f/n",&sweep_period);
       fscanf(stream2, "%f/n",&sweep_step);
       fscanf(stream2, "%f/n",&temp_sp1);
       fscanf(stream2, "%f/n",&temp_band1);
       fscanf(stream2, "%f/n",&temp_pbmul1);
       fscanf(stream2, "%f/n",&temp_inmul1);
       fscanf(stream2, "%f/n",&temp_dermul1);
       fscanf(stream2, "%f/n",&press_sp1);
       fscanf(stream2, "%f/n",&press_band1);
       fscanf(stream2, "%f/n",&press_pbmul1);
       fscanf(stream2, "%f/n",&press_inmul1);
       fscanf(stream2, "%f",&press_dermul1);

    temp_sp=(double)temp_sp1;
    temp_sp=100.0685*((0.0039076*temp_sp)+1);
    temp_sp_change=(double)temp_sp1;

    temp_band=(double)temp_band1;

    temp_pbmul=(double)temp_pbmul1;

    temp_inmul=(double)temp_inmul1;

    temp_dermul=(double)temp_dermul1;

    press_sp=(double)press_sp1;
    press_sp=100.0685*((0.0039076*press_sp)+1);

    press_band=(double)press_band1;

    press_pbmul=(double)press_pbmul1;

    press_inmul=(double)press_inmul1;
```

```
    press_dermul=(double)press_dermul1;

    fclose(stream2);
}


          /*******************************/
          /*   Temperature Sweep Routine  */
          /*******************************/

void change_temp_setpoint(void)

{
    temp_sp_change=temp_sp_change+(double)sweep_step;
    temp_sp=temp_sp_change;
    temp_sp=100.0685*((0.0039076*temp_sp)+1);
}

void reverse_sweep(void)
{
  sweep_step=-1*sweep_step;
}




          /*****************************/
          /* Sweep Stage Temp Control */
          /*****************************/


void control_temp(void)
{
    temp_e[1]=temp_sp-temp_ac;

    temp_pb=temp_pbmul*temp_e[1];

    temp_inn=(temp_inmul*temp_e[1])*(double)(t[1]-t[0]);
    temp_in[1]=temp_in[0]+temp_inn;


    temp_der=(temp_e[1]-temp_e[0])/(double)(t[1]-t[0]);
    temp_der=temp_dermul*temp_der;
```

```
    if(fabs(temp_der) > temp_band) temp_der = temp_band;

    temp_out=temp_pb+temp_in[1]+temp_der;
    if(temp_out>temp_band) temp_out=temp_band;
    if(temp_out<0) temp_out=0;


     outpw(CARDNUMBER+ICRO, DAI);
     outpw(CARDNUMBER+IDNRO, ADC);
     outpw(CARDNUMBER+AWCRO+SHOB, 1);
     outpw(CARDNUMBER+ARCRO, DAAD);
     outpw(CARDNUMBER+AWRO, (int)temp_out);


    temp_e[0]=temp_e[1];
    temp_in[0]=temp_in[1];

}

          /*******************************/
          /* Reference Stage Temp Control */
          /*******************************/

void control_press(void)
{
    press_e[1]=press_sp-press_ac;

    press_pb=press_pbmul*press_e[1];

    press_inn=(press_inmul*press_e[1])*(double)(t[1]-t[0]);
    press_in[1]=press_in[0]+press_inn;

    press_der=(press_e[1]-press_e[0])/(double)(t[1]-t[0]);
    press_der=press_dermul*press_der;
    if(fabs(press_der) > press_band) press_der =
press_band;

    press_out=press_pb+press_in[1]+press_der;
    if(press_out>press_band) press_out=press_band;
    if(press_out<0) press_out=0;

     outpw(CARDNUMBER+ICRO, DAI);
     outpw(CARDNUMBER+IDNRO, ADC);
     outpw(CARDNUMBER+AWCRO+SHOB, 0);
```

```
     outpw(CARDNUMBER+ARCRO, DAAD);
     outpw(CARDNUMBER+AWRO, (int)press_out);

    press_e[0]=press_e[1];
    press_in[0]=press_in[1];

 }


              /*************************/
              /*  Dispaly Setup Routine */
              /*************************/
void setup_screen(void)
{
 _clearscreen(_GCLEARSCREEN);
 _settextposition(3,9);
 _outtext("SET POINT:");
 _settextposition(4,7);
 _outtext("TEMPERATURE:");
 _settextposition(5,1);
 _outtext("CONTROLLER OUTPUT:");
 _settextposition(6,1);
 _outtext("PROPORTIONAL GAIN:");
 _settextposition(7,2);
 _outtext("INTEGRATOR RESET:");
 _settextposition(8,3);
 _outtext("DERIVATIVE RATE:");
 _settextposition(9,8);
 _outtext("RESISTANCE:");
 _settextposition(10,13);
 _outtext("ERROR:");

 _settextposition(3,48);
 _outtext("SET POINT:");
 _settextposition(4,46);
 _outtext("TEMPERATURE:");
 _settextposition(5,40);
 _outtext("CONTROLLER OUTPUT:");
 _settextposition(6,40);
 _outtext("PROPORTIONAL GAIN:");
 _settextposition(7,41);
 _outtext("INTEGRATOR RESET:");
 _settextposition(8,42);
 _outtext("DERIVATIVE RATE:");
```

```
 _settextposition(9,47);
 _outtext("VOLTAGE:");
 _settextposition(10,52);
 _outtext("ERROR:");
/*
 _settextposition(11,62);
 _outtext("FLOW RATE 1:");
 _settextposition(12,62);
 _outtext("FLOW RATE 2:");
 _settextposition(13,67);
 _outtext("DIFFERENCE:");
*/

}

              /*************************/
              /* Output Data to Display */
              /*************************/

void output_data(void)
   {

     char buffer[80];
     _settextwindow(0,20,15,30);
     _clearscreen(_GWINDOW);
     sprintf(buffer,"%.4f",temp_sp_change);
     _settextposition(3,0);
     _outtext(buffer);

     sprintf(buffer,"%.4f",temp);
     _settextposition(4,0);
     _outtext(buffer);

     sprintf(buffer,"%.4f",temp_out);
     _settextposition(5,0);
     _outtext(buffer);

     sprintf(buffer,"%.4f",temp_pb);
     _settextposition(6,0);
     _outtext(buffer);

     sprintf(buffer,"%.4f",temp_in[1]);
     _settextposition(7,0);
     _outtext(buffer);
```

```
sprintf(buffer,"%.4f",temp_der);
_settextposition(8,0);
_outtext(buffer);

sprintf(buffer,"%.4f",temp_ac);
_settextposition(9,0);
_outtext(buffer);

sprintf(buffer,"%.4f",temp_e[1]);
_settextposition(10,0);
_outtext(buffer);

_settextwindow(0,59,15,75);
_clearscreen(_GWINDOW);

sprintf(buffer,"%.4f",press_sp1);
_settextposition(3,0);
_outtext(buffer);

sprintf(buffer,"%.4f",press);
_settextposition(4,0);
_outtext(buffer);

sprintf(buffer,"%.4f",press_out);
_settextposition(5,0);
_outtext(buffer);

sprintf(buffer,"%.4f",press_pb);
_settextposition(6,0);
_outtext(buffer);

sprintf(buffer,"%.4f",press_in[1]);
_settextposition(7,0);
_outtext(buffer);

sprintf(buffer,"%.4f",press_der);
_settextposition(8,0);
_outtext(buffer);

sprintf(buffer,"%.4f",press_ac);
_settextposition(9,0);
_outtext(buffer);
```

```
      sprintf(buffer,"%.4f",press_e[1]);
      _settextposition(10,0);
      _outtext(buffer);
    /*
      sprintf(buffer,"%.4f",flow_a);
      _settextposition(11,0);
      _outtext(buffer);

      sprintf(buffer,"%.4f",flow_b);
      _settextposition(12,0);
      _outtext(buffer);

      sprintf(buffer,"%.4f",diff_flow);
      _settextposition(13,0);
      _outtext(buffer);

      */

     if(ttrip<t[1])
      {

           /* Print data to ptout.dat file */
           fprintf(stream1, "%.4f   %.4f   %.4f    %.4f
%.4f    %.4f\n", temp, press, flow_a, flow_b, diff_flow,
t[1]);
           ttrip=ttrip+60;
      }
    }



              /************************/
              /* Read Sweep Stage Temp */
              /************************/
double rdrtd(void)
     {
       int i,rtd;
       double res;
       char rstring[19];
          rtd = ibfind("fwrtd");
          ibwrt(rtd, "F2R1S3T1B1I1Q0", 14);
          ibrd( rtd, rstring, 18 );
          for(i=0; i<4; i++) rstring[i]=' ';
          rstring[17]=0x00;
```

```
        res=(double)atof(rstring);
        return (res);
    }


        /*****************************/
        /* Read Reference Stage Temp */
        /*****************************/

double rdpress(void)
    {
        int i,rtd;
        double res;
        char rstring[19];
        rtd = ibfind("twrtd");
        ibwrt(rtd, "F2R1S3T1B1I1Q0", 14);
        ibrd( rtd, rstring, 18 );
        for(i=0; i<4; i++) rstring[i]=' ';
        rstring[17]=0x00;
        res=(double)atof(rstring);
        return (res);
    }
```

```
□
                /*********************/
□
                /* Read Flow Meter a */
□
                /*********************/
double rdflow_a(void)
     {
        int i,rtd;
        double res;
        char rstring[19];
          rtd = ibfind("brone");
          ibwrt(rtd, "F0R1S3T1B1I1Q0", 14);
          ibrd( rtd, rstring, 18 );
          for(i=0; i<4; i++) rstring[i]=' ';
          rstring[17]=0x00;
          res=(double)atof(rstring);
          return (res);
     }



                /*********************/
                /* Read Flow Meter b */
                /*********************/
double rdflow_b(void)
     {
        int i,rtd;
        double res;
        char rstring[19];
          rtd = ibfind("brtwo");
          ibwrt(rtd, "F0R1S3T1B1I1Q0", 14);
          ibrd( rtd, rstring, 18 );
          for(i=0; i<4; i++) rstring[i]=' ';
          rstring[17]=0x00;
          res=(double)atof(rstring);
          return (res);
     }


void graph_flow_diff(long number, double value, double
value1)
{
```

```
long i,h;
double Min, Max, Min1, Max1;
buffer2[number]=value1;
buffer[number]=value;
findminmax(buffer, flow_a, flow_b, &Min1, &Max1,&Min,
&Max);

     _setcolor(1);
     _rectangle(_GFILLINTERIOR, 0,244,639,479);
     _setcolor(15);
     _rectangle(_GBORDER, 0,244,639,479);
     if (Min == Max) Max++;
     _moveto(1,479-(int)(((float)buffer[1]-
(float)Min)*140.0f/(float)(Max-Min)));

     for(i=1;i<=number;i++)
          {
               _setcolor(15);

     _lineto(1+(int)((float)i*240.0f/(float)number), 478-
(int)(((float)buffer[i]-(float)Min)*140.0f/(float)(Max-
Min)));

          }
     if (Min1 == Max1) Max1++;
     _moveto(1,479-(int)(((float)buffer2[1]-
(float)Min1)*140.0f/(float)(Max1-Min1)));
     for(h=1;h<=number;h++)
          {
               _setcolor(10);

     _lineto(1+(int)((float)h*240.0f/(float)number), 478-
(int)(((float)buffer2[h]-(float)Min1)*140.0f/(float)(Max1-
Min1)));
          }
}

void findminmax(double *buffer, double value, double
value1, double *Min1, double *Max1, double *Min, double
*Max)

{
     long r,j;
```

```
     *Min1 = (*Max1=buffer2[0]);
     *Min = (*Max = buffer[0]);
     for (r=1; r<value; r++);
          {
               if (*Min > buffer[r] ) *Min =buffer[r];
               if (*Max < buffer[r] ) *Max = buffer[r];
                    }
     for (j=1; j<value1; j++);
          {
               if (*Min1 > buffer2[r] ) *Min1 =buffer2[r];
               if (*Max1 < buffer2[r] ) *Max1 =buffer2[r];

          }
}
```

REFERENCES

1. Forbes, R.J., "More Studies in Early Petroleum History: 1860-1880," E.J. Brill, Leiden, Netherlands, 1959.

2. Grues, W.A., and Stevens, D.R., "Chemical Technology and Petroleum," McGraw-Hill Book Company Inc., New York, 1960.

3. McClaflin, E.G., and Whitfill, D.L., J. Pet. Tech., **36** 1965 (1984).

4. Son, A.J, Graugnard, R.B., and Chai, B.J., "Proceedings of the 1993 International Symposium on Oilfield Chemistry," Society of Petroleum Engineers, Richardson, TX, 1993, p351.

5. Bos, B., and vanden Haak, K., Proc. Indo. Petro. Assoc., **6** (1980).

6. Corney, J.D., "Advancements in the Use of Magnetics for Controlling Deposits and BS&W in Oil Wells," Southwest Petroleum Short Course, Texas Tech Univ., Lubbock, TX (1993).

7. Padgett, F.W., Hefley, D.G., and Henriksen, A., Ind. Eng. Chem., **18** 832 (1926).

8. Buchler, C.C., and Graves, G.D., Ind. Eng. Chem., **19** 718 (1927).

9. Rhodes, F.H., Mason, C.W., and Sutton, W.R., Ind. Eng. Chem., **19** 935 (1927).

10. Katz, J., Inst. Pet. Tech., **18** 37 (1932).

11. Ferris, S.W., and Cowles, H.C., Ind. Eng. Chem., **37** 1054 (1945).

12. Clarke, E.W., Ind. Eng. Chem., **43** 2526 (1951).

13. Edwards, R.T., Ind. Eng. Chem., **49** 750 (1957).

14. Misra, S., Baruah, S., and Singh, K., SPE Proc. and Fac., **2** 50 (1995).

15. Hamouda, A.A., and Viken, B.K.,"Proceedings of the 1993 International Symposium on Oilfield Chemistry," Society of Petroleum Engineers, Richardson, TX, 1993, p385.

16. Niesen, V., "Flow Assurance Issues Reference Library," Multiphase Solutions Inc., Ponca City, OK, 1998.

17. Szostak, R.J., Chem. Proc., **9** 8 (1985).

18. John, J., and Haberman, W.L., "Introduction to Fluid Mechanics," Prentice Hall, New Jersey, 1988.

19. Thermistors, "The Temperature Handbook," Omega Engineering Inc, Stanford, CT, 1995.

BIOGRAPHICAL SKETCH

Johnny Lamar Evans Jr. is the son of Johnny Lamar Evans Sr., obviously, and Peggy Mae Evans and was born on June 20, 1970. Born in Slidell, Louisiana, his family moved after his birth, this would become a typical occurrence about every two to three years.

The son of a retired military officer, Johnny had many opportunities to travel and see the world. From the mid-70s until 1986, he spent most of his life in West Germany. After a lifetime of world traveling and many moves, the author's family moved to Hinesville, Georgia, where Johnny graduated from high school in 1988.

The author attended Mercer University from 1988-1990, appearing to pursue a general education certificate. Thankfully, a romantic relationship and eventual engagement helped to focus his attention on a degree. With his wife by his side, he moved to Milledgeville, Georgia, and completed his B.S. in chemistry in December of 1993. In 1994, they moved to Gainesville, Florida, where he began his graduate work under the supervision of Dr. Samuel

Colgate. He poured his life into his teaching duties, which paid off with great awards, and eventually into the study of wax deposition in petroleum pipelines.

I certify that I have read this study and that in my opinion it conforms to acceptable standards of scholarly presentation and is fully adequate, in scope and quality, as a dissertation for the degree of Doctor of Philosophy.

Samuel O. Colgate

Samuel O. Colgate, Chair
Professor of Chemistry

I certify that I have read this study and that in my opinion it conforms to acceptable standards of scholarly presentation and is fully adequate, in scope and quality, as a dissertation for the degree of Doctor of Philosophy.

Luis M. Muga
Professor of Chemistry

I certify that I have read this study and that in my opinion it conforms to acceptable standards of scholarly presentation and is fully adequate, in scope and quality, as a dissertation for the degree of Doctor of Philosophy.

Alex Angerhofer
Associate Professor of Chemistry

I certify that I have read this study and that in my opinion it conforms to acceptable standards of scholarly presentation and is fully adequate, in scope and quality, as a dissertation for the degree of Doctor of Philosophy.

Carl R. Stouffer
Professor of Chemistry

I certify that I have read this study and that in my opinion it conforms to acceptable standards of scholarly presentation and is fully adequate, in scope and quality, as a dissertation for the degree of Doctor of Philosophy.

Gar B. Hoflund

Gar Hoflund
Professor of Chemical Engineering

This dissertation was submitted to the Graduate Faculty of the Department of Chemistry in the College of Liberal Arts and Sciences and to the Graduate School and was accepted as partial fulfillment of the requirements for the degree of Doctor of Philosophy.

August 1998

Dean, Graduate School